6-2005

High Temperature Chemical Degradation of PMR-15 Polymer Resins

Grant W. Robinson

HIGH TEMPERATURE CHEMICAL DEGRADATION OF PMR-15 POLYMER RESINS

THESIS

Grant W. Robinson, Ensign, USNR

AFIT/GAE/ENY/05-J09

DEPARTMENT OF THE AIR FORCE
AIR UNIVERSITY
AIR FORCE INSTITUTE OF TECHNOLOGY

Wright-Patterson Air Force Base, Ohio

The views expressed in this thesis are those of the author and do not reflect the official policy or position of the United States Navy, the United States Air Force, Department of Defense, or the United States Government.

AFIT/GAE/ENY/05-J09

HIGH TEMPERATURE CHEMICAL DEGRADATION OF PMR-15 POLYMER RESINS

THESIS

Presented to the Faculty

Department of Aeronautics and Astronautics

Graduate School of Engineering and Management

Air Force Institute of Technology

Air University

Air Education and Training Command

In Partial Fulfillment of the Requirements for the

Degree of Master of Science in Aeronautical Engineering

Grant W. Robinson

Ensign, USNR

June 2005

AFIT/GAE/ENY/05-J09

HIGH TEMPERATURE CHEMICAL DEGRADATION OF PMR-15 POLYMER RESINS

Grant W. Robinson
Ensign, USNR

Approved:

_____	_____
Professor Anthony N. Palazotto (Chairman)	date
_____	_____
Professor Marina B. Ruggles–Wrenn (Member)	date
_____	_____
Professor Theodore Nicholas (Member)	date

Abstract

PMR-15 is a polymer resin for glass and carbon reinforced composites used for high temperature, civilian and military aerospace applications. The harsh environments of PMR-15 applications lead to long term structural degradation and, in turn, impact the readiness capabilities of the system. This study investigated the thermal and oxidative degradation of PMR-15 neat resin powder through the use of thermal gravimetric analysis (TGA) in oxygen, argon and air at isothermal hold temperatures of 260, 288, 316, and 343 °C for 250 hours. The TGA measured the degradation by recording the change in neat resin powder mass versus time. The qualitative results were similar for all tests. The specimens initially lost weight at a rapid rate followed by a reduction in the weight loss rate to a near constant value that was dependent upon the isothermal temperature and the gaseous environment. The data from these tests will be used by researchers in the Air Force Research Laboratory Materials and Manufacturing Directorate to further efforts made towards developing a constitutive law and the associated models to predict the behavior of polymer matrix reinforced composites.

Acknowledgements

I would like to thank my thesis advisor, Dr. Anthony Palazotto, for his assistance and guidance through out my thesis project. His counseling was vital to keeping me on task and effective. I would also like to thank Dr. Greg Schoeppner and the AFRL Materials and Manufacturing Directorate for funding this research. Moreover, without Dr. Schoeppner's personal guidance along the way, I would not have been able to complete this project within the short time I had and for that I am grateful. In addition to the rest of the individuals in the Materials and Manufacturing Directorate, I would like to give a special thanks to Bill Price for his assistance in teaching me how to perform tests using the TGA. I owe Tara Storage special thanks as well because she allowed me to monopolize the TGA with such long duration tests and thus pushed back her own tests.

In addition, I would like to thank my family for their continuous support and belief in my abilities. Knowing that my mother was always urging me to push myself and make the most of every opportunity has been a great help through this project. Lastly, I would like to thank the fellow Navy classmates. The advice and wisdom from the more senior students kept me grounded and constantly advancing. Without the help from my peers, both inside and outside of the classroom, I would not have been able to successfully complete this work.

Grant W. Robinson

Table of Contents

Page

List of Figures

Page

Page

List of Tables

HIGH TEMPERATURE CHEMICAL DEGRADATION

OF PMR-15 POLYMER RESINS

I. Introduction and Literature Review

Background

High-Temperature Polymer Matrix Composites, HTPMC's, are of ever increasing area of interest to many different industries. They can provide significant advantages over corresponding metallic components due to their low density and high specific strength (1). Within the aerospace industry, system weight is of the utmost importance and as a result, PMC's have found application in aircraft engines, airframes, missiles, rockets and other weight sensitive systems. Meador (1) reports that one kilogram reduction in the weight of an aircraft engine can provide an overall weight reduction in the entire aircraft of as much as twenty kilograms. This type of benefit can be realized by the ability to increase a vehicle's range, payload, and or performance. Material technology with these capabilities becomes very important to the military research efforts.

Various aerospace and aero-propulsion applications such as turbine engines, exhaust wash structures and high-speed aircraft skins result in components being exposed to harsh service conditions. In these applications PMC's, particularly polyimide composites, have the ability to retain their mechanical properties at elevated temperatures (2). PMR-15, of the Polymerization of Monomeric Reactant (PMR) family of polyimides, shown in Figure 1, was developed in the 1970's at the NASA Lewis Research Center and is regarded as one of the most widely used high-temperature, thermosetting polyimide

resins used in aircraft engine components. Its popularity can be attributed to its ease of processing, low cost, good stability, and performance at temperatures up to 288 °C (3).

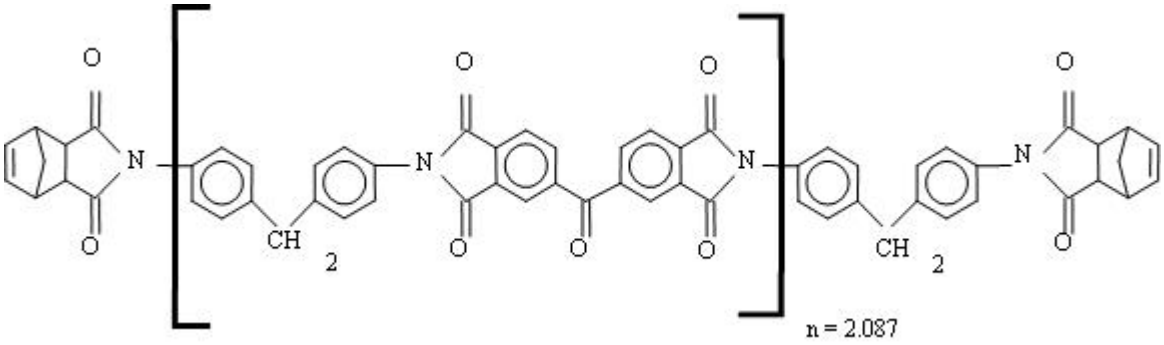

Figure 1: Stoichiometry of PMR-15 Resin ($MW_{theorectical}$ = 1500)

The benefits of PMC's come at the cost of finite lifetimes that are dictated, not by fatigue as many metallic components are, but by aging effects that are primarily driven by environmental degradation. Degradation is defined in this thesis as nonreversible chemical changes that result in reduced mechanical performance of a system, either neat resin or a fiber/matrix composite.

It is generally agreed upon that temperature and oxygen diffusion and its subsequent chemical interaction are the principal factors in degradation. Their combined aging effects, thermo-oxidation, give rise to corrosion, surface stresses, and micro-cracking. These effects manifest themselves in reduced mechanical performance of the system (4).

By understanding the mechanisms of degradation, the polyimide family of PMC matrices can be re-designed or new types developed, in order to provide longer useful lives that match the design life of a particular airframe which can extend from 18000 to 30000 hours (5). In addition, a more directly tangible benefit could be reduced life cycle costs of aircraft systems through reduced replacement parts and maintenance.

Organic Polymer Matrix Aging

Overview

The aging of composite materials is considered a process that modifies the structure of the material on both the microscopic and molecular levels. The altered material structure can most readily be characterized by changes in the material's mechanical properties. Because of this relationship, the aging of composites can be monitored and investigated by researching the mechanical properties of materials in different environments. Excluding mechanical loading, the parameters that are most important to the aging process are time and environment (4). Time is independent; however the environment can be controlled. The environmental variables can include temperature, moisture, gaseous molecular make-up and pressure, temperature being the most important. For PMR-15/graphite composites, only the matrix is affected as graphite fiber degradation is negligible for the applicable temperatures. However, because the matrix supports and protects the fibers, the aging that occurs in the matrix has a direct impact on the properties of the composite system. It is clear that composite aging is a multidisciplinary event, but it may be broken apart and modeled independently by ignoring some of the coupled effects of loading (4). There are two types of aging that act to degrade the composite: physical aging and chemical aging.

Physical Aging

Physical aging is considered a process that modifies the material on the macro- and microscopic levels. The structural organization of the molecules in space may be altered, but the molecular structure of the material remains unchanged. Internal stresses within a composite can lead to physical aging (4). These stresses may have been a result

of thermal expansion differentials between the reinforcing fibers and the matrix or the result of residual stresses from the manufacturing process. The micromechanical damage caused by fatigue can also give rise to physical aging effects as well. For most polyimides, physical aging is not reversible through annealing of the material. These types of physical aging can eventually give rise to micro-cracking in the matrix ultimately reducing the mechanical performance of the system. However, this is not to say that composite cracking is due solely to physical aging. Composite aging is typically a combined result of physical and chemical aging (4).

Chemical Aging

Chemical aging, the type of aging that this thesis investigated, is that which modifies the chemical structure of the polymer through mechanisms such as reticulation, depolymerization, elimination, and substitution and is typically an irreversible type of aging (4). Those mechanisms are primarily a result of chemical reactions between the polymer matrix and the elements that make up the environment. The temperature alone modifies the polymer and it also drives the reaction rates for the various reactions that occur between the polymer and the environmental elements. Chemical aging can further be divided into two types of degradation: hygrothermo-oxidation and volume aging.

Chemical Aging Mechanisms

Thermo-oxidation and Surface Layer Development

Thermo-oxidation describes the effects of the polymer reacting with the oxygen present in the aging environment. The changes in the molecular structure that occur during oxidation result in a reduction in molecular weight as a result of chemical bond breakage, microrupturing and the outgassing of low molecular weight oxidation by-

products that can be quantified as a local mass loss (6). Because the rate of chemical reaction is controlled by the reaction temperature, the effect of oxygen on the composite is temperature dependent. The degradation starts at the surface of the polymer and advances inward as oxygen diffuses into the structure. However, due to the fact that the rate of reaction is much greater than the rate of diffusion for PMR-15 resin, the degradation becomes diffusion limited (7). Thermo-oxidation acts to create a surface layer in the matrix resin that has different chemical and mechanical properties than the original, unaged material. Figure 2 is a photomicrograph, taken from Ripberger et al (6), of PMR-15 neat resin after aging. Marais et al (4) added that this layer ultimately reaches a maximum thickness that rarely exceeds 0.2 mm even in severe thermo-oxidative environments. However, this is not to say that the oxidation layer advancement has stopped. Conversely, the layer continues to advance inward but its thickness remains constant because the effect of thermo-oxidation also eventually breaks down the outer surface of oxidized layer at a rate equal to that of the oxidized layer's front. The continued reduction in size makes a clear case that thermo-oxidation and its effects are very important to composite material applications.

In general, research has revealed that the oxidized surface layer has different mechanical properties when compared to the core material. These changes include decreased tensile strength, strain to failure, flexural strength, and density and increased moduli when compared to the unoxidized interior resin (7). Bowles et al (8) reported that for thin composites, less than eight plies, the thin oxidized surface layer had significant effects on the compression properties of the material.

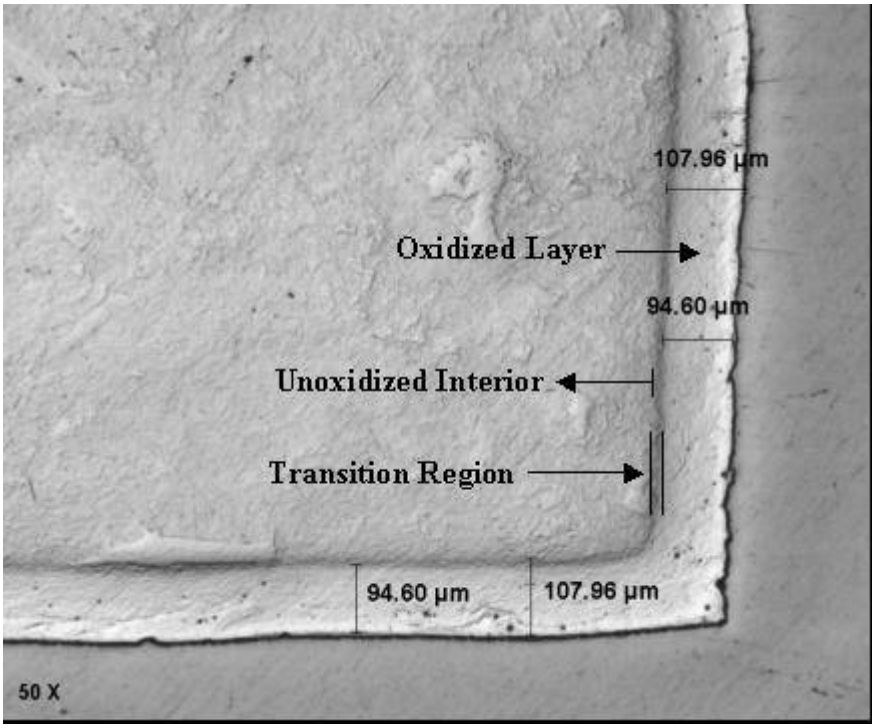

Figure 2: Photomicrograph of oxide layer formation, transition region, and unoxidized interior of PMR-15 after 196 hrs of aging at 343 °C (6)

Volume Aging of the Resin

The chemical make up of the PMR-15 polymer is also altered simply by sustained exposure to elevated temperatures. The volume aging (chemical changes not associated with oxidation), as it will be referred to in this thesis, has the effect of degradation and consolidation of the molecular structure whereby parts of the polymer chains break creating free radicals. A free radical is an atom or molecule that has an unpaired electron in its outer shell. These changes are the result of the material seeking a thermodynamic equilibrium at the given temperature. The increase in free radicals makes the resin increasingly unstable as the free radicals have a higher propensity to react in order to fill their outer shells. These reactions within the core material are changing the polymer chain. The extent of volume aging may be quantified by tracking the variation of the glass transition temperature (Tg). Initially, volume aging is similar to polymer post-

curing in that consolidation occurs in the matrix and additional cross-linking takes place. The process then transitions to more of a degradation through random chemical bond breakage in the polymer chain as the energy levels of the bonds are exceeded and they break producing the free radicals. The mechanical effect of volume aging tends to modify the load transfer properties between the fibers thus affecting the overall visco-elastic behavior of the composite (4).

Combined Effects of Chemical Aging

The combined effect of volume and thermo-oxidative aging reduces the usable life of organic polymer composites. The differing mechanical properties between the oxidized surface layer and the unoxidized, but aged, core material create an additive degradation effect. The oxidized layer has been found to be stiffer and have a different coefficient of thermal expansion than the core material (6). Through thermal cycling and isothermal aging, the surface layer shrinks thus creating strain variations between the fibers, core material and oxidized surface layer that ultimately result in microcracking of the matrix material. These cracks provide a new path for oxygen to diffuse further into the polymer resulting in the advancement of the oxidized surface layer and further material loss into the core material as shown in Figure 3 (8).

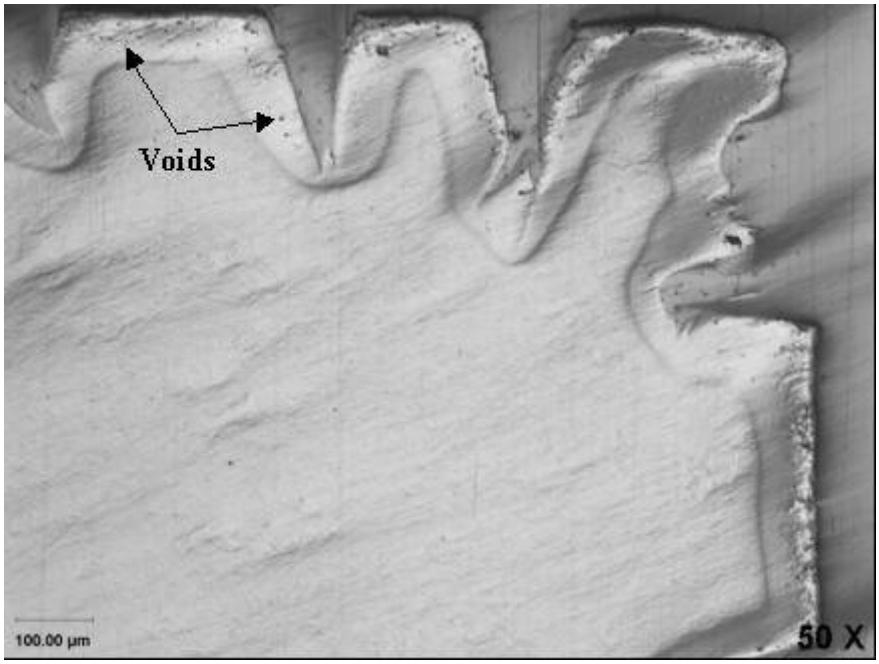

Figure 3: Severe surface damage of PMR-15 as a result of isothermal aging at 343 °C for 640 hrs in air (6)

PMR-15 Literature Review

Composites Systems: Fibers and the Polymer Matrix

Bowles (9) researched the oxidized surface layer thickness, weight loss and compression properties of graphite reinforced PMR-15 4, 8, and 20 ply composite panels at 204, 260, 288, 316, and 343 ºC for durations up to 18,000 hours. He found that a simple, linear relationship exists between the compression strength and the oxidized surface layer thickness that developed during the high temperature isothermal aging. He concluded that although the surface layer thickness was indicative of the reduced compression strength, the core material is the main contributor to the strength reduction. In addition to the linear relation between the compression strength and the surface layer thickness, the surface layer thickness was also linearly related to the aging time for each temperature. For the 4 ply panels, some tests indicated that the oxidized surface layer

extended almost entirely through the panel significantly reducing its compression properties.

Bowles (9) found that the weight loss of T650-35/PMR-15 composite samples could be divided into three phases as shown in Figure 4. The first phase from the origin to Point A is characterized by rapid weight loss that is proportional to the specimen volume. The rate of weight loss then reduces to a linear rate between A and B before accelerating as a result of microcracking and exposed fiber oxidation mainly along the cut surfaces at times after Point B.

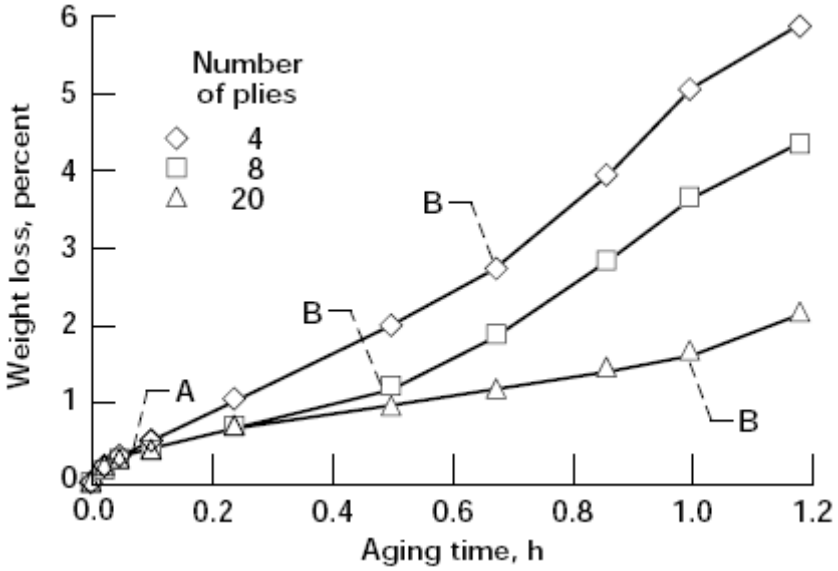

Figure 4: Weight loss of T650-35/PMR-15 composites as a function of aging time at 316 °C (10)

Bowles et al (11) investigated the effect of different fiber surface treatments (termed sizing) on carbon fiber/PMR-15 composites' mechanical and thermo-oxidative stability after isothermal aging at 316 ºC for 240, 500 and 1000 hr. They found that the sizing, which determined the fiber/matrix bonding, had an effect not only on the mechanical properties of the composite, but also on its thermo-oxidative stability. The composite with the lowest level of bonding measured by the interlaminar shear strength, untreated Hercules A-carbon fiber AU-4/PMR-15, exhibited a weight loss that was twice

that of the AS-4 and AS-4G treated-fiber composites. Their weight loss analysis revealed the highest rates of weight loss at 240 hr for all of the fibers. Bowles et al believed that the higher initial weight loss rate was the release of reaction products that had not diffused out of the composite during curing and post-curing. The rate of weight loss decreased at 500 hr while the oxidized surface layer was forming and advancing inward. During the time between 500 and 1000 hr, the rate of loss became nearly constant for the treated fibers. The AU-4 untreated fiber composite experienced cracking along the specimen cut edges that resulted in an increased weight loss rate when measured at 1000 hr.

Chung et al (12) similarly found that the fibers have an effect on degradation. They performed weight loss experiments on carbon fiber/epoxy laminates using various fiber directions and lay-up sequences. They compared the degradation, measured by weight loss, of composite specimens with unidirectional fibers in the longitudinal direction and the transverse direction and composite specimens with cross-ply lay-up sequences. They found that degradation was an anisotropic phenomenon where the weight loss increased with the surface to volume ratio. Moreover, the oxidation preferentially occurred along the fiber direction as opposed to a direction transverse to the fiber axis. This conclusion indicates that thermo-oxidative degradation should be considered to be a tensorial quantity (position and orientation dependent) as opposed to a scalar quantity as it is when quantified solely through weight loss. Chung et al also introduced and validated the concept of 'Equivalent Cycle Time' as a characteristic isothermal degradation time at a specific temperature that produced the same mechanical property changes as a cyclic thermo-mechanical application would produce. This

principle provides a method for more accurately correlating laboratory test results with that which would occur in real applications.

Neat Resin Research: Polymer Matrix Alone

Meador et al (13) researched the chemical mechanisms that caused the weight loss of PMR-15 imidized neat resin and found that the end-caps of the molecular chain accounted for much of the weight loss of the resin aged in air at elevated temperatures. They tracked the type of reactions by Carbon-13 labeling the end caps and then performing nuclear magnetic resonance (NMR) spectroscopy. Because Carbon-13 has an unpaired neutron in its nucleus it has a nuclear spin that can be detected with NMR techniques, thus allowing the tracking of the end-cap paths of degradation. Two paths were found. Both of the paths lead to the production of biradicals (two unpaired electrons present on the molecule) that react with oxygen, but the paths differ in the type of biradical that is formed on the end- cap and the ultimate reaction by-products. The important result of their research found that one path corresponded to greater weight loss than the other. They proposed that new end-caps that more strongly favor the lower weight loss degradation process could lead to polymers that experience less shrinkage and cracking in the oxidized layer thus slowing the overall degradation process.

Research by Xie et al (14) used a Thermo-gravimetric analyzer coupled with a Fourier-Transform Infrared (FTIR) spectrometer to determine the degradation products released as PMR-15 and other polyimides were heated to 950 °C at 1 °C/min in nitrogen. They found that H_20, CO, CO_2, CH_4, and NH_4 were the major degradation products.

Patekar (15) also investigated the degradation products of PMR-15 resin. He found similar results to Xie et al (14) with the major species including Carbon Monoxide,

Carbon Dioxide, and Water. He further identified Carbon Dioxide as the most prevalent species released at temperatures below 350 °C.

Bowles et al (8) conducted isothermal weight loss studies at four temperatures (204, 260, 288, and 316 ºC) with PMR-15 imidized neat resin and composites in air. His two primary research points were to investigate the role of oxygen in the thermo-oxidative degradation of the composites and to track the dimensional changes that accompany composite aging. He found that the effects of aging are dependent upon the exposure time and the location within the specimens. Two visibly distinct regions within the specimens were identified: a visibly undamaged core underneath a visibly damaged surface layer. Bowles et al also found that three different phenomena were taking place during the degradation process through weight loss analysis. There is a small weight gain, a small slightly temperature-dependent weight fraction bulk material weight loss, and a large temperature-dependent fractional weight loss originating in the visibly damaged surface layer of the material. At temperatures above 260 ºC, the surface weight loss exceeded the other weight change mechanisms. At temperatures below 260 ºC, the bulk weight loss and surface loss became more equivalent. Between 175 and 260 ºC, the weight gain phenomenon decreased as the aging temperature increased. The finite temperature range when weight gain mechanism is observable is due to the fact that at higher temperatures its effect is masked by the weight loss mechanisms of the bulk material and the surface material. At temperatures above 316 ºC, Bowles et al found differing rates of weight loss during different periods of time of a single experiment. Similar to Bowles previous work (11), they found a high initial rate of weight loss attributed to the release of reaction products not released during the curing and post-

curing, a lower rate of weight loss due to volume and thermo-oxidative aging, and then an accelerated rate caused by microcracking that had exposed new area to the oxygen present in the test environment.

Tsuji et al (16), Johnson et al (17), and Ripberger et al (6) all investigated the mechanical properties of the oxidized surface layer and unoxidized interior material. All of the investigations found the same distinct regions that Bowles et al (8) found: a visibly oxidized surface layer and a visibly unoxidized core material. Ripberger et al and Johnson et al further identified a reaction zone that existed between the oxidized outer surface layer and the interior core material.

Tsuji et al (16) degraded PMR-15 in air and nitrogen at 316 ºC for durations up to 800 hours. Four point bend tests of unoxidized specimens and specimens with an oxidized surface layer were used to determine the elastic moduli of the oxidized surface and the interior material. Furthermore, bimaterial strip specimens consisting of the oxidized surface material and the unoxidized core material were constructed in order to determine the surface layer shrinkage and the coefficients of thermal expansion (CTE). These tests concluded that the oxidized material had different mechanical properties with respect to the unoxidized material. The shrinkage of the surface layer is restrained by the core, resulting in tensile stresses, which are increased by the elevated modulus. The difference in the CTE and stiffness help to explain the surface cracking that is observed in air-aged specimens.

Johnson et al (17) used an atomic force microscope (AFM) to make nanoindentation measurements in order to study the extent of the aging time and temperature effects on oxidized PMR-15 neat resin. In specimens aged at 316 ºC for up to

344 hours, they found that the elastic modulus was constant from the surface to a certain depth and the oxidized surface layer thickness increased with the aging time. They determined that this layer can be considered homogeneously oxidized and is representative of a zero order reaction (the diffusion of oxygen was not the controlling parameter). Beneath the oxidized layer, the modulus decreased further into the material finally arriving at the modulus of the unaged material. This reaction zone was believed to be representative of a first order reaction (the diffusion of oxygen was the controlling parameter and thus limiting the rate of reaction). Specimens aged at 343 ºC for up to 324 hours, exhibited modulus profiles that indicated the absence of a diffusion independent zone and only a diffusion controlled zone. Johnson et al reinforced the conclusion that the surface and core had notably different mechanical properties that were dependent on aging temperature and time.

Ripberger et al (6) used nanoindentation, optical microscopy, and thermomechanical analysis to investigate the differing properties of aged PMR-15 neat resin. Their tests included specimens aged for 1000 hours at 343 ºC in air and in an oxygen-depleted environment by sealing the specimen in a stainless steel bag (the steel bag reduced the amount of oxygen by consumption). The nanoindentation revealed a similar modulus profile to that which was found by Johnson et al (17). As the aging time increased, the thickness of the oxidized layer grew continuously but approached an asymptote. However, the elastic modulus of the oxidized layer and the thickness of the transition region remained relatively constant. Testing also revealed that the modulus of the aged, unoxidized interior material was slightly greater than the modulus of the unaged PMR-15 resin. The optical measurements of the oxidation layer thickness and the active

reaction zone thickness were found to agree with the boundaries of the three regions identified by the nanoindentation data.

Scope of project

Modeling Efforts of Air Force Research Laboratory Materials and Manufacturing Directorate

The current design methodology for aerospace structural systems includes the assumption that the polymer matrix composite material is considered 'chemically static', thus disregarding the fact that chemical/physical degradation occurs, changing the physical properties (7). In order to more appropriately design composite systems, one must be able to predict the long-term stiffness and strength as well as the potential failure mechanisms. The construction of models that can predict these properties has been the focus of many researchers in the composites community.

The focus of AFRL Materials and Manufacturing Directorate modeling efforts is two fold: 1) to understand changes in the polymer properties with service environment exposure; and 2) to accurately model these changes in the appropriate constitutive model that will be integrated in micro-mechanics models (7). The actual chemical processes that are responsible for the polymer matrix degradation and its subsequent reduction in mechanical performance are very complex and it would be impractical to track the changes on a quantum mechanics level. However, through the use of semi-empirical methods the micro-mechanical effects of the chemical degradation and the material's behavior can be modeled on the continuum level. To this end, AFRL researchers are performing tests on PMR-15, a widely used polymer matrix, and AFR-PE-4, a newly developed polymer matrix, to determine the rates of oxidation and the spatial variability

of the oxidized surface layer mechanical properties as a function of aging. The results of these efforts will be used as inputs to model the oxygen diffusion kinetics and the polymer oxidation to predict the evolution of the oxidation surface layer. This model will then be combined with models that predict other polymer behaviors to form a complete constitutive polymer model that can be integrated into the micro-mechanics models. This process of building up models is termed hiearchical modeling and is diagrammatically shown in Figure 5. The ultimate goal as mentioned above is to predict the long-term stiffness and strength as well as potential failure mechanisms. For this reason, the hiearchical model will ultimately include three-dimensional ply-level analyses to represent the anisotropic behavior of potential polymer matrix composite applications.

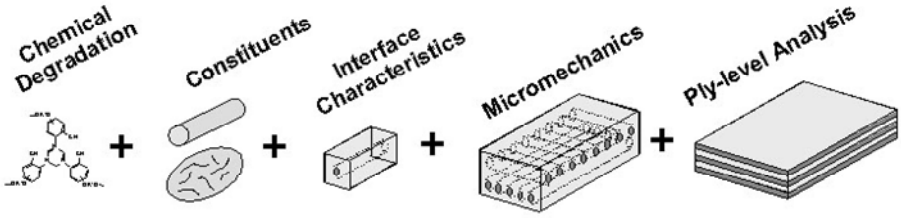

Figure 5: Hiearchical Modeling concept (7)

One such model predicts the concentration and reaction of oxygen as it diffuses into the surface of PMR-15 at 288 and 343 C. The concentration is then related to the rate of oxygen consumption thus determining the advancement of the oxidized layer into neat resin. The model, developed by Pochiraju and Tandon (18), combines a Fickian diffusion model with a term to account for the reduction in concentration as a result of consumption through reaction with the polymer. With C(x, y, z; t) representing the oxygen concentration field at any time within a domain with a diffusivity of D_{ij} and a consumptive reaction with a rate R(C), the diffusion-reaction with orthotropic diffusivity is given by Eq. (1)

$$\frac{\partial C}{\partial t} = \left(D_{11} \frac{\partial^2 C}{\partial x^2} + D_{22} \frac{\partial^2 C}{\partial y^2} + D_{33} \frac{\partial^2 C}{\partial z^2} \right) - R(C) \tag{1}$$

With the following boundary conditions

$C^s = SP$ on the exposed boundries

C^s: Boundry Sorption

S : Solubility

P : Partial Pressure

$\frac{dC}{dt} = 0$ on symmetry boundries

For PMR-15, the diffusivity was assumed to be isotropic thus simplifying the equation. The diffusivity was also assumed to be temperature dependent and modeled by an Arrhenius-type form where E_a is an activation energy and D_0 is a pre-exponent.

$$D_{ij} = D_0 e^{\left(\frac{-E_a}{RT}\right)} \tag{2}$$

The consumptive reaction term R(C) was defined by a saturation reaction rate (R_0) modified by a function f (C) developed by Abdeljaoued (19) that describes the reduction in availability of oxygen for consumption when the saturation concentration is not reached.

$$R(C) = R_0 f(C) \tag{3}$$

$$f(C) = \frac{2\beta C}{1+\beta C}\left[1 - \frac{\beta C}{2(1+\beta C)}\right] \tag{4}$$

The abscissa of concentration dependence reaction model Eq. (4) has a normalized concentration parameter, βC, in which, β, nondimensionalizes the concentration field for a specific temperature. The value of β was determined from weight loss data at comparable temperatures in environments with different partials pressures of oxygen.

The saturation reaction rate (R_0) was determined experimentally through the use of an active reaction zone analogy. The active reaction zone is the region over which oxygen has diffused and is reacting with the polymer. The thickness of this zone is indicative of the saturation reaction rate. The rate was temperature dependent and modeled by an Arrhenius-type relation, Eq. (5), where R_0* and R_a are the scaling and activation constants.

$$R_0 = R_0^* e^{\left(\frac{-R_a}{RT}\right)} \tag{5}$$

The oxidation layer thickness and reaction rate are related by a proportionality constant (α) in the manner shown in Eq. (6) below.

$$\frac{dW}{dt} = \alpha R(C) \tag{6}$$

Furthermore, an oxidation state parameter (ϕ) was defined as the current weight of the material divided by the original, unoxidized weight of the material at a given point and time. Hence,

$$\frac{d\phi}{dt} = \frac{dW}{dt} \tag{7}$$

Combining Eq. (6) and Eq. (7)

$$\frac{d\varphi(t)}{dt} = \alpha R(C) \tag{8}$$

This relation (Eq. (8)) determined the state of oxidation at a depth in the material with respect to time. A reaction completion value of the oxidation state variable (ϕ_{ox}) was calculated from weight loss data and used to quantify the transition value of the oxidation state parameter (ϕ) at which a point in the polymer matrix became completely oxidized material.

The results of the Pochiraju and Tandon model predicted the growth of the oxidized surface layer with relatively good precision based on simple linear and age independent relationships. Their model was highly dependent on experimental data and the indirect relationships, the most critical being the proportionality constant (α). The final model utilized a linear variation of the proportionality constant for the first 40 hrs of simulation and then a constant value of (α) thereafter.

Focus of this Thesis

The focus of this thesis was to generate new weight loss data that could be used to refine AFRL Materials and Manufacturing Directorate sponsored models currently under development such as the Pochiraju and Tandon model described in the previous section. This was done by examining the thermo-oxidative degradation of PMR-15 neat resin imidized powder through weight loss measurements. In conjunction with the thesis's sponsor, Dr. Greg Schoeppner of the AFRL Materials and Manufacturing Directorate at Wright-Patterson Air Force Base, the following test matrix, shown in Table 1, was developed in this continuing endeavor.

Temperature (°F)	Temperature (°C)	Argon	Air	Oxygen
650	343	X	X	X
600	316	X	X	X
550	288	X	X	X
500	260	X	X	X

Specimen Size: 10 mg ± 1 mg
Test Duration: 250 hours

Table 1: PMR-15 Neat Resin Powder Test Matrix

The table laid out 12 tests, 4 temperatures for each environment: air, argon, and oxygen. Each test was run for 250 hours (15000 min) or until the specimen's normalized weight reached a horizontal asymptote as indicated by a weight loss rate of less than 0.002 % per hour. The weight of the specimen was measured and recorded by the TGA

PC Software as a function of time in an isothermal hold. The data was exported and analyzed using Microsoft® Office Excel.

In this thesis, the normalized weight (M/M_0) is used to present and quantify the degradation state of PMR-15 neat resin powder. Weight loss can be expressed in various forms that combine the initial weight (M_0) and transient weight (M): normalized weight ($W = M/M_0$), extent of weight loss ($L = 1- M/ M_0$), and total weight loss ($T = M_0 – M = L M_0$). These forms are converted to one another with the known initial weight. Normalized weight was chosen because it is the default method with which the test apparatus used to display data. Where the rate of weight loss was presented, it was expressed as a positive change in normalized weight per hour ($R = (W_t - W_{t+1}) / \Delta t$).

The decision to perform testing on powdered resin was arrived at from a desire to eliminate the potentially limiting effect that diffusion can have on the observed weight loss rate. In this manner, the observed reaction rates, characterized by specimen weight loss, could be considered zero order reactions (diffusion independent) as defined by Johnson et al (17).

The Pochiraju and Tandon weight loss dependent model parameters, saturation reaction rate (R_0), normalized concentration parameters (β), and proportionality constants (α) were evaluated for comparison to the previously used values. However, the calculated parameters were not direct replacements for the currently used parameters because the model was written based on bulk polymer aging where diffusion does become limiting in the case for PMR-15 neat resin.

Additionally, the use of Time-Temperature Superposition, a principle borrowed from Linear-Viscoelastic Theory, was evaluated as a method to extend the results of this

testing so that the data can be applied at any aging temperature within the bounds presented in Table 1.

II. Materials, Equipment, and Experimental Procedure

Material History and Processing

The PMR-15 neat resin used was manufactured and supplied to this research effort by the Air Force Research Laboratory's Materials and Manufacturing Directorate. High purity PMR-15 imidized foam (the precursor to cured PMR-15 resin) was purchased from Cytec Industries, Inc. and crushed into powder using a hydraulic press. Neat resin panels measuring 11.68 cm by 15.24 cm and an average thickness of 0.23 cm made from the PMR-15 imidized powder were compression molded in a steel die mold with nonporous Teflon® coating. The cured PMR-15 neat resin was then post-cured in air at atmospheric pressure for 16 hours at 343 °C. The fully prepared plaques were cut using a diamond wet-saw and distilled water (for cooling) into asymmetrical pieces approximately 5.0-8.0 cm in both length and width. The PMR-15 pieces were then cleaned with a common dishwashing soap and dried with standard paper towels. Once dried, the pieces were placed in a vacuum oven at 105 °C for a minimum of two days to allow for all moisture to be removed.

The PMR-15 powder was generated using a five step process created by ENS Susan Mendenhall to support her PMR-15 resin research. The photos and process were taken from her master's thesis (2). The process yielded a particle size of 45-90 μm. The five steps in the process were: Pre-cutting the PMR-15 pieces, crushing the PMR-15 into fragments, milling the crushed pieces into powder, sifting the powder into 45- 90 μm particle sizes, and removing the impurities in the powder through suspension.

The PMR-15 neat resin was cut from the stored sample size into 3 gram solid pieces as shown in Figure 6. The specimens were further reduced in size using shears resulting in randomly shaped 1 mm to 5 mm pieces that could be effectively crushed in a press. Breaking the larger samples into random sizes and shapes helped to facilitate the further crushing of the sample once it was placed in the press. In Figure 7, the smaller pieces are shown on the left of the larger PMR-15 resin piece from where they originated.

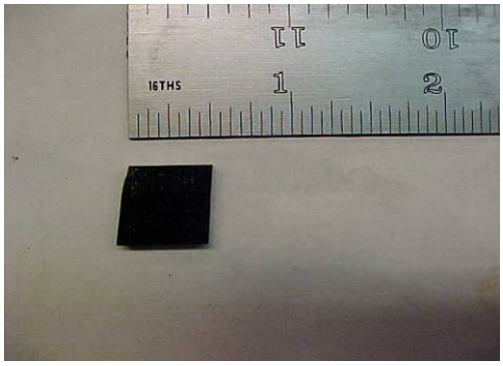

Figure 6: 3.0 g Solid Sample of PMR-15 (2)

Figure 7: Broken Pieces of PMR-15 (2)

The 1 to 5 mm fragments were placed between two stainless steel plates approximately 6.0 x 10.0 x 1.0 in. in size and the assembly was placed in the center of a Wabash 30 Ton Press, shown in Figure 8. The press was ramped up to its maximum pressure at the time of use (28,000 psi) crushing the fragments. Once the press reached its maximum force, it was retracted and the plates were removed. The crushed PMR-15

particles were rearranged between the plates and then the process was repeated two more times. The final results, shown in Figure 9, were fragment sizes that would be milled into a powder by a ball mill.

Figure 8: Wabash 30 Ton Press (2)

Figure 9: Pressed PMR-15 resin fragments (2)

The pressed PMR-15 resin fragments were milled in a Crescent WIG-L-BUG ball mill, shown in Figure 10. Twenty milligram portions of the fragments were milled for one hour and then emptied into a set of sieves. The ball mill yielded a powder with the desired particle size of approximately 45- 90 µm despite not being designed for samples as hard as PMR-15 (compression strength 60-70 MPa).

The powder was sifted through two 6” diameter stainless steel ASTM test sieves. The 90 µm sieve was stacked on top of the 45 µm sieve, which were both stacked on top of a collection pan, as shown in Figure 11. The particles that collected in the 45 µm sieve were removed for use. The particles that passed through the 45 µm sieve were collected in the collection pan and discarded. The powder that did not pass through the 90 µm sieve was collected and then placed back into the mill until the desired particle size was obtained. Figure 12 and Figure 13 show are pictures taken under a microscope of the PMR-15 powder unsifted and sifted, respectively.

Figure 10: WIG-L-BUG Ball Mill, Front and Side Views (2)

Figure 11: 90 µm Sieve, 45 µm Sieve, and Collection Pan (2)

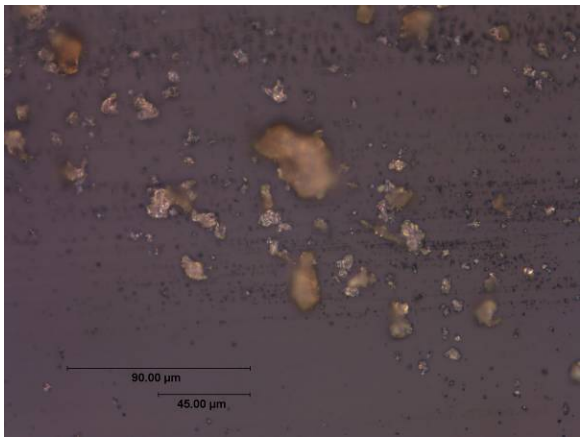

Figure 12: Unsifted PMR-15 Particles, 40X (2)

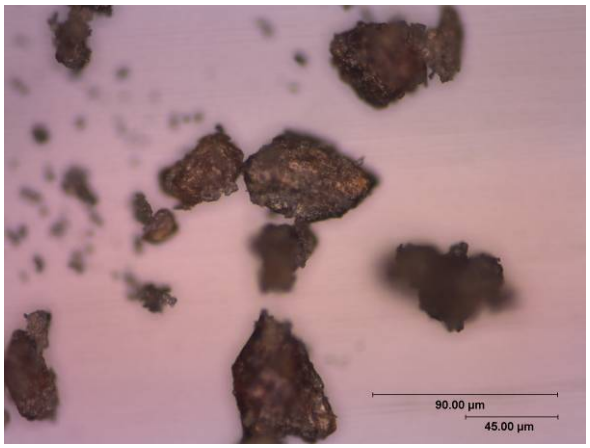

Figure 13: Sifted PMR-15 Particles, 40X (2)

The final step in the process involved removing impurities such as metal debris resulting from the milling process and other contaminants from the powder by suspension in carbon tetrachloride. The density difference between PMR-15, 1.30 g/cm^3 (20), and carbon tetrachloride, 1.59 g/cm^3 (21), allowed the all of the metallic and other denser contaminants to be separated from the PMR-15. The PMR-15 that settled on the surface of the solution was poured off into a glass container and the carbon tetrachloride was allowed to evaporate out. After drying, the PMR-15 neat resin powder was collect in a glass container and stored in a nitrogen purged dessicator storage unit.

Laboratory Test Equipment

Thermo-Gravimetric Equipment

TA Instruments Thermo-Gravimetric Analyzer

The thermal testing was carried out using a TA Instruments Hi-Resolution TGA-2950 Thermo-Gravimetric Analyzer, shown in Figure 14. The TGA records the weight of a specimen as a function of time and temperature in a controlled gas environment. After calibration, the TGA can accurately record the weight of a specimen to 0.001 mg ± 0.1% for a maximum specimen weight of 1.0 g. During testing the specimens are weighed in a 50 μL platinum basket that is attached to the balance mechanism. The machine is designed to carry out experiments in Air, Argon, Helium, Nitrogen, or Oxygen at sustained temperatures between 25 °C up to 1000 °C for indefinite periods of time. Experiments can be designed to include multiple isothermal hold temperatures and rates of heating from 0.1 to 100 °C per min. Each experiment and heating method is created using the associated PC software.

Figure 14: Thermo-gravimetric Analyzer

Cahn Thermo-Gravimetric Analyzer

Thought was given to utilizing another currently unallocated thermo-gravimetric analyzer to prevent other in-house AFRL projects from falling behind due to equipment unavailability. The sponsoring laboratory also owned a CAHN TGA shown in Figure 15. This apparatus could perform the same tests as the TA Instruments TGA on even larger specimens and was currently not being utilized in any research efforts. Unfortunately, a comparison of the results for similar tests conducted at 316 °C for 45 hr did not match. Figure 16 shows that the weight fractions differed by nearly 20 % at the conclusion of the tests. It was decided that the remaining tests would have to be completed on the more accurate TA Instruments TGA.

Figure 15: Cahn Thermo-Gravimetric Analyzer

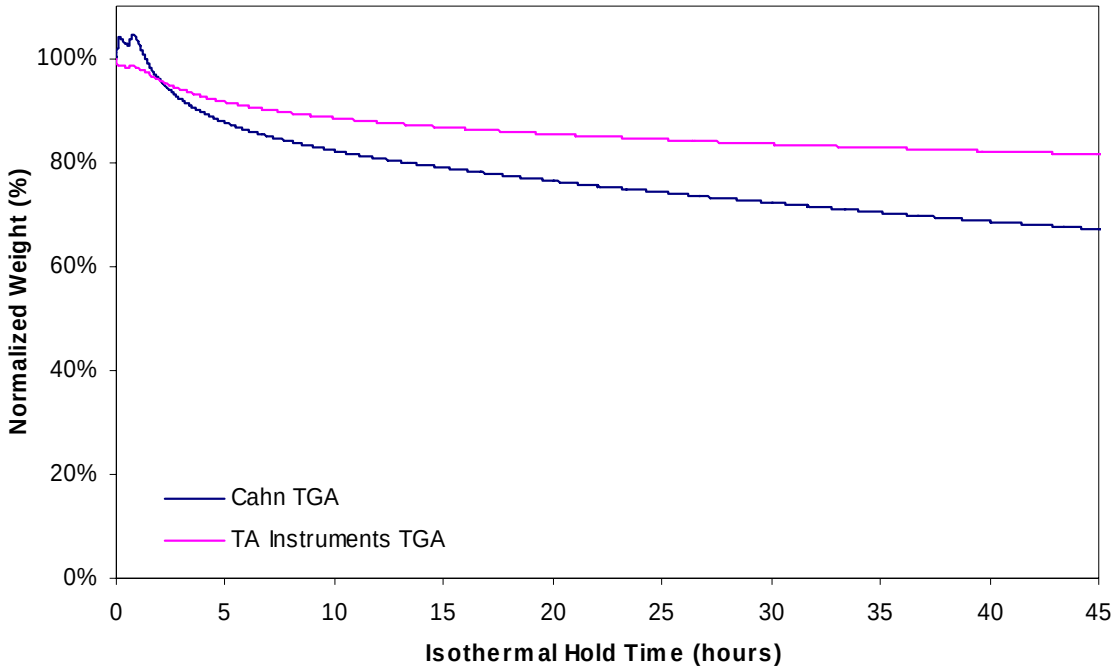

Figure 16: Cahn TGA Comparison Test to TA Instruments TGA

PMR-15 Powder in Air at 316 °C for 45 hours

Purge Gas Supply Systems

Both TGAs require an external supply of purge gas for the balance chamber and the furnace where the specimen is located. The purge gas is used to establish the desired aging environment around the specimen and to remove any gaseous degradation products from the test environment. The purge gas flow must be maintained at 100 cc/min or less being distributed with 40 % to the balance chamber and 60 % to the furnace. This ratio is required to prevent degradation products from traveling up into the balance chamber and contaminating the sensing mechanism. An Omega Flowmeter, visible in Figure 17, was used to maintain the correct flow rates. For tests in air, house air was used and regulated by the flowmeter. The tests requiring oxygen and argon dictated the use of bottled gas. Pressure regulators were used to reduce tank pressure to a flow regulator inlet pressure of 10 psi. The use of oxygen further required the use of stainless steel gas lines. Because

pure oxygen had never been used in this machine only plastic hoses had been installed and thus had to be replaced. A new stainless steel supply system was fabricated and arranged so that the supply cylinders could be rapidly changed out when a different purge gas was required. Figure 17 shows the new system.

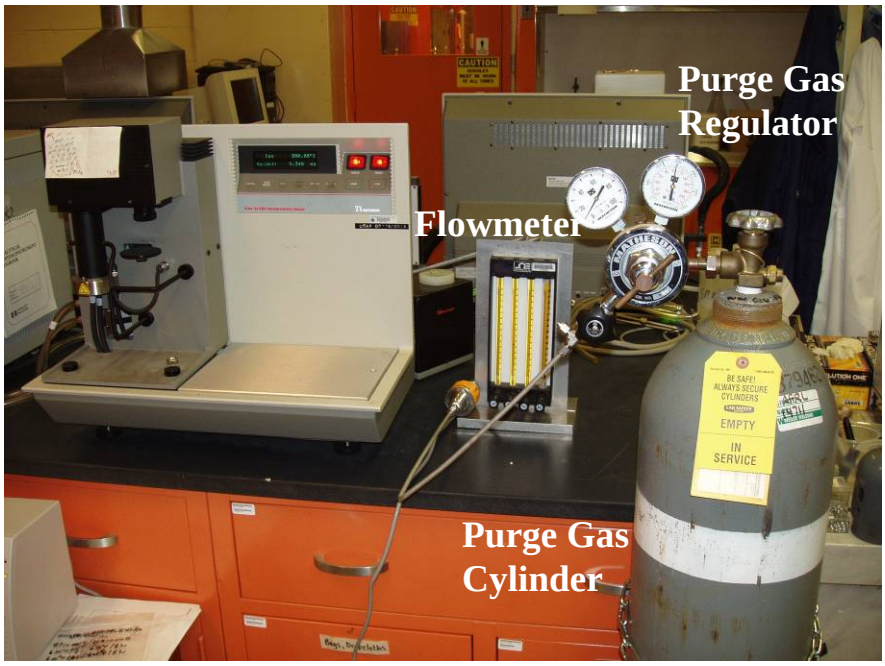

Figure 17: Stainless steel gas supply system TGA

Experimental Procedure

This section reviews the details of how individual tests were performed for this research effort. As with any scientific balance, the TGA must first be tared in order to insure accurate measurement of only the test specimen. Through taring the balance, the TGA records the weight of the platinum basket and accounts for that weight so when the sample is placed in the basket, the recorded weight is only due to the test specimen. In order to insure accurate taring, the platinum basket must be cleaned. The cleaning was accomplished by heating the basket with a Butane Torch until it reached a completely dull, orange glow indicating that any residue from previous experiments had been burned off. The clean basket was loaded into the TGA for the taring process. The purge gas

system was then lined up to provide the required flow and desired gas. Five minutes was generally allowed to pass after the furnace was sealed to allow the test purge gas to completely replace the air that occupied the furnace while it was open. Having established the proper test environment in the furnace, the taring process was initiated with the "Tare" button on the TGA. The actual taring process was internal to the machine and required no operator input beyond loading the clean basket and establishing the purge gas flow.

The TGA was controlled through its associated software on a PC locate in the lab. The experimental parameters must be set up prior to starting the actual data acquisition. This step was completed while the TGA was taring. The required input parameters include: specimen type, purge gas, a heating method, and the data file storage name. The heating parameters are in a file that tells the TGA what heating rates, isothermal hold temperatures, and hold durations to use in a particular test. The heating program used for each test in this thesis started with a heating rate of 20 °C per minute up to 110 °C where it would hold for 2 hours. This intermediate hold was designed to allow any moisture present in the powder to evaporate and its actual duration was less than 2 hours as will be explained below. This intermediate hold temperature was followed by a ramp up to the isothermal test temperature. The final isothermal test temperatures for each test are shown in the test matrix show in Table 1. The heating rate for the final ramp was 100 °C per minute, the maximum ramp rate for the TGA, in order to minimize weight lost at temperatures other than the test temperature. At this point, the software was ready to initiate the test. Once the TGA had completed its internal taring process, a specimen was loaded.

The final step before starting the test was to load the PMR-15 test specimen into the TGA. The platinum basket was placed on a Mettler AM100 electronic balance and tared. A 10 mg (± 1 mg) PMR-15 powder specimen was measured into the basket. The specimen and basket were then placed on the loading tray and loaded into the TGA as shown in Figure 18 and Figure 19. Once the basket was loaded, the furnace was sealed. Again, five minutes was allowed for the purge gas (house air, argon, or oxygen) to displace the ambient air from the furnace and then test was initiated through the PC software.

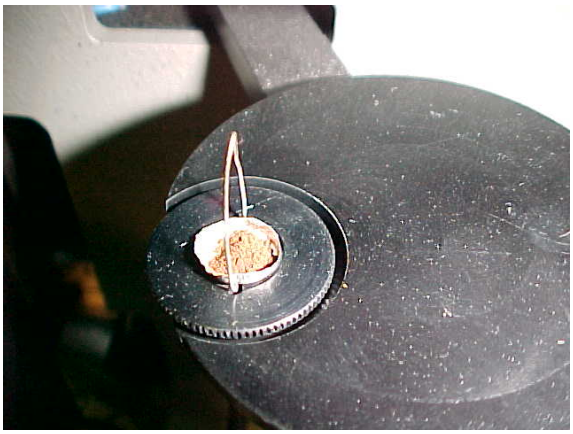

Figure 18: Loading the Platinum Basket

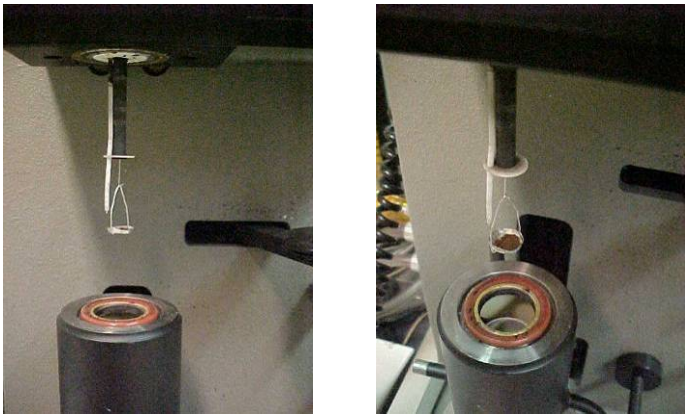

Figure 19: TGA Loaded with Platinum Basket with PMR-15 Sample

The TGA started the heating procedure by ramping up to 110 °C and then holding. During the entire test, the PC software provided real time output for continuous observation by the operator. For all tests, the normalized weight (M/M_0) dropped rapidly indicating the loss of absorbed moisture from the loading procedure. After this rapid drop, an average of seven minutes from the test start and two minutes at 110 °C, the normalized weight reached relatively constant value. Approximately ten more minutes at 110 °C was allowed to assure that all of the absorbed moisture had evaporated at which time the operator overrode the programmed heating method and manually advanced the TGA to the next segment, the ramp up to the final test temperature. Overshoot was minimized by the TGA by internally regulation of the ramping rate.

The tests were concluded automatically by the TGA after 250 hours of aging or manually by the operator if the normalized weight reached a horizontal asymptote as indicated by a weight loss rate of less than 0.02 % per hour. The TGA shut down and saved the data in either case. After the TGA furnace had cooled, the PMR-15 specimen was removed and discarded.

Time-Temperature Superposition Theory and Application

Visco-Elastic materials properties, such as creep compliance, are time dependent and often require long-duration tests. Traditionally, accelerated testing has been accomplished through the application of Time-Temperature Superposition. At the core of the methodology, is the fact that certain visco-elastic phenomenon will occur more rapidly at higher temperatures. Therefore, by testing at an elevated temperature, a longer duration test can be effectively accelerated. The difficulty with accelerating the tests in

this manner is establishing a relationship between the accelerated test and an otherwise unaccelerated test (22).

The application of Time-Temperature Superposition is based on the assumption that the observed behavior can be modeled with an Arrhenius-type relation. In the Pochiraju and Tandon model, the saturation reaction rate (R_0) is assumed to have that type of relationship as shown in Eq. (9).

$$R_0 = R_0^* e^{\left(\frac{-R_a}{RT}\right)}$$
$$R_0^* : \text{Scaling Constant} \quad (9)$$
$$R_a : \text{Activation Constant}$$

Furthermore, when diffusion is considered negligible (reason for testing powdered PMR-15 neat resin), the rate of weight loss can be assumed proportional to the saturation reaction rate.

The process of Time-Temperature Superposition for creep compliance begins with compliance measurements at different temperatures over a short period of time and plotted against the log of time. The data from different temperatures are then shifted on the log time scale such that a single master curve is created as shown in Figure 20. The shift factor (A_t) required to align individual curves with the master curve defines the relationship between the horizontal shift and the temperature. Using the master curve shifted to the respective elevated temperature, the creep compliance can be predicted over a larger range of time than was actually tested (22).

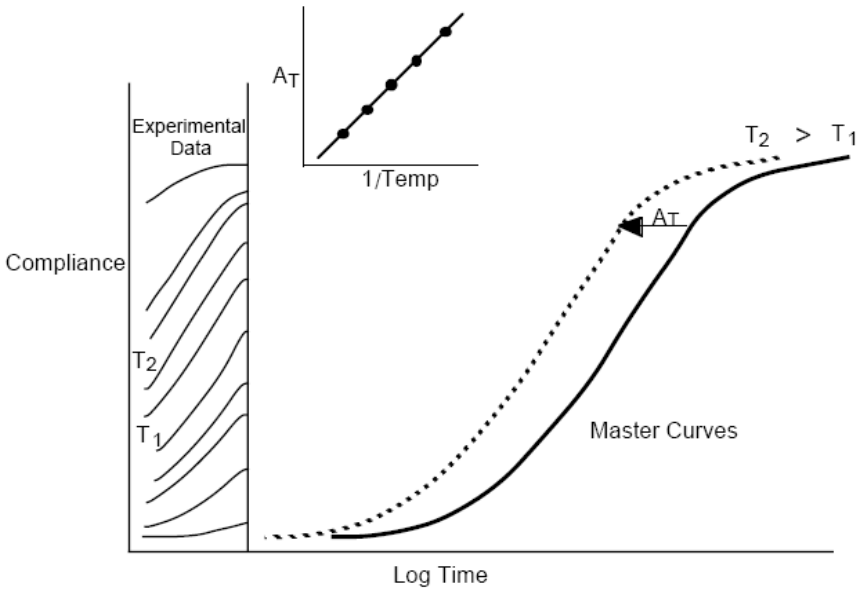

Figure 20: Time-Temperature Superposition and the formation of a master curve (22)

In this thesis, the normalized weight for each test within a single gas was plotted versus the log of time in minutes. One temperature, typically the highest tested, was selected as the master curve and shift factors (A_t) were used to shift the remaining temperatures along the log time scale such that all of the data collapsed to a single curve. For polymers at temperatures below their glass transition temperature (Tg), Eq. (10) defines the relationship that was used to relate the shift factor to the temperature (22).

$$\log\left(A_t\right) = \eta\left(\frac{1}{T} - \frac{1}{T_0}\right) \tag{10}$$

The shift rate (η) is determined by plotting the log of the shift factor (A_t) versus the difference between the inverse of the master curve temperature (T_0) and the tested temperature (T). This relationship was predicted based on the assumed Arrhenius-type relation that defined the saturation reaction rate (R_0). If the assumption is correct, then the shift rate (η) will be a constant and the master curve can be used to extend the results of this thesis to temperatures within the range outlined in Table 1.

III. Results and Analysis

Overview

The results of the PMR-15 neat resin powder aging are discussed in this chapter. Table 2 shows the tests that were actually completed from Table 1 during this research effort.

Table 2: PMR-15 Neat Resin Completed Tests

Temperature (°F)	Temperature (°C)	Argon	Air	Oxygen
650	343	X	X	X
600	316	X	X	X
550	288	X	X	X
500	260		X	

TGA Results in Air

General Trends

The tests in air were completed first during this research. Table 3 presents a summary of the numeric results and Figure 21 presents the normalized weight as a function of time for all four test temperatures.

Table 3: Summarized Test Results in Air

Test Temperature (°C)	**260**	**288**	**316**	**343**
Initial Weight (mg)	9.933	9.847	10.382	10.847
110 °C Hold Time (min)	22	26	27	18
Moisture Content (%)	0.6%	1.4%	1.6%	0.8%
Final Weight (mg)	8.618	7.779	6.97	2.528
Final Normalized Weight (%)	86.76%	79.00%	67.14%	23.31%
Linear Weight Loss Rate (%/hr)	0.024%	0.027%	0.061%	0.242%
Linearity Transition Time (hr)	165	160	130	50

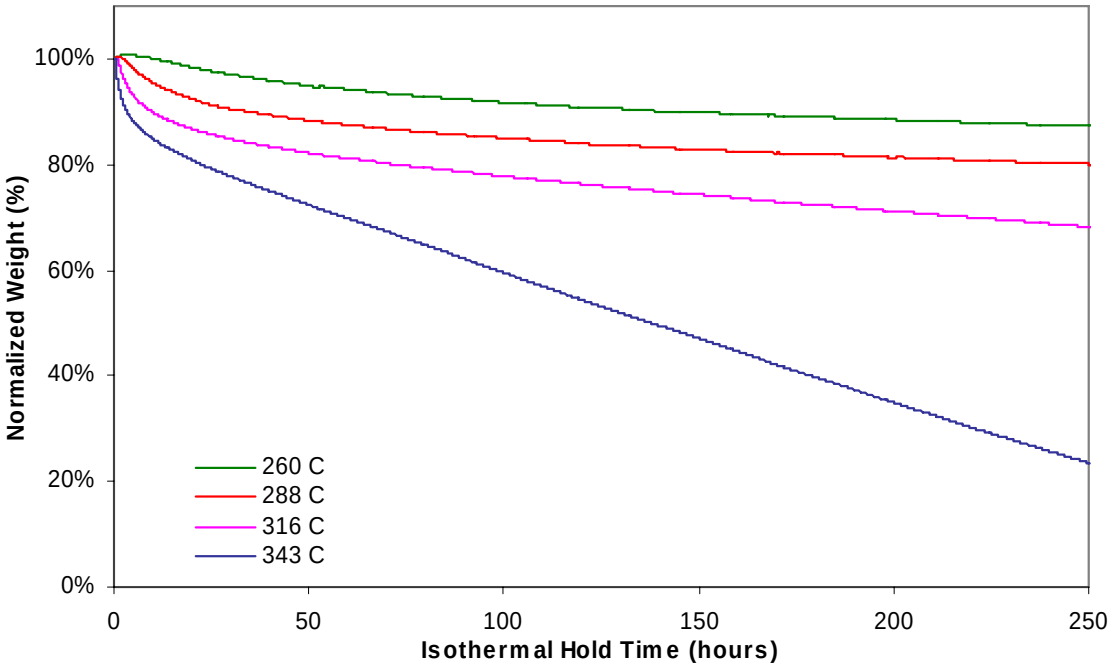

Figure 21: TGA of PMR-15 Neat Resin Powder in Air

For all of the tested temperatures it was noted that the normalized weight dropped rapidly and then approached a near constant rate of weight loss. The high initial rate of weight loss may be attributed to the release of reaction products that had not diffused during curing and post-curing cycles as suggested by Bowles et al (8). Another possible source of the high initial rate may be smaller particles completely oxidizing very rapidly in the early stages of testing. As can be seen in Figure 13, particles smaller than 45 μm were still present after the sifting process. The increased number of smaller particles effectively increases the area available to react thus increasing the initial rate of weight loss. The duration of the accelerated weight loss was also very temperature dependent lending itself to either theory for the accelerated initial rate.

The steep decrease in normalized weight then transitioned to a lower rate of weight loss and finally to a near constant rate of weight loss. The precise time at which the near constant rate was reached was subjective and heavily dependent upon the

temperature as well. The transition time can be approximated more easily by plotting the slope of the normalized weight over time. The time at which the slope of the rate of change becomes zero is the time when the normalized weight loss rate became constant. Figure 22 presents the normalized rate of weight loss per hour as a function of time. Recall that the rate of normalized weight loss is defined as ($R = (W_t - W_{t+1}) / \Delta t$).

The original data contained large transients caused by purge air flow fluctuations that cluttered the plot making interpretation and presentation difficult. As a result, the data used in Figure 22 is the running average rate over a 5 hour period. The normalized weight loss plot, Figure 21, does not show the same noise because of the different scale used to present the data. An undesirable result of the large averages used in weight loss rate calculations was the creation of longer than actual transient durations. The circled trough in Figure 22 is an example. There was transient point near a normalize weight loss rate of -0.1% and when points within 5 hours of it were averaged, they were all equally shifted by it. The plot of the unsmoothed rates of weight loss can be viewed in Appendix A in Figure 45. Despite the complication, the trends can be readily identified.

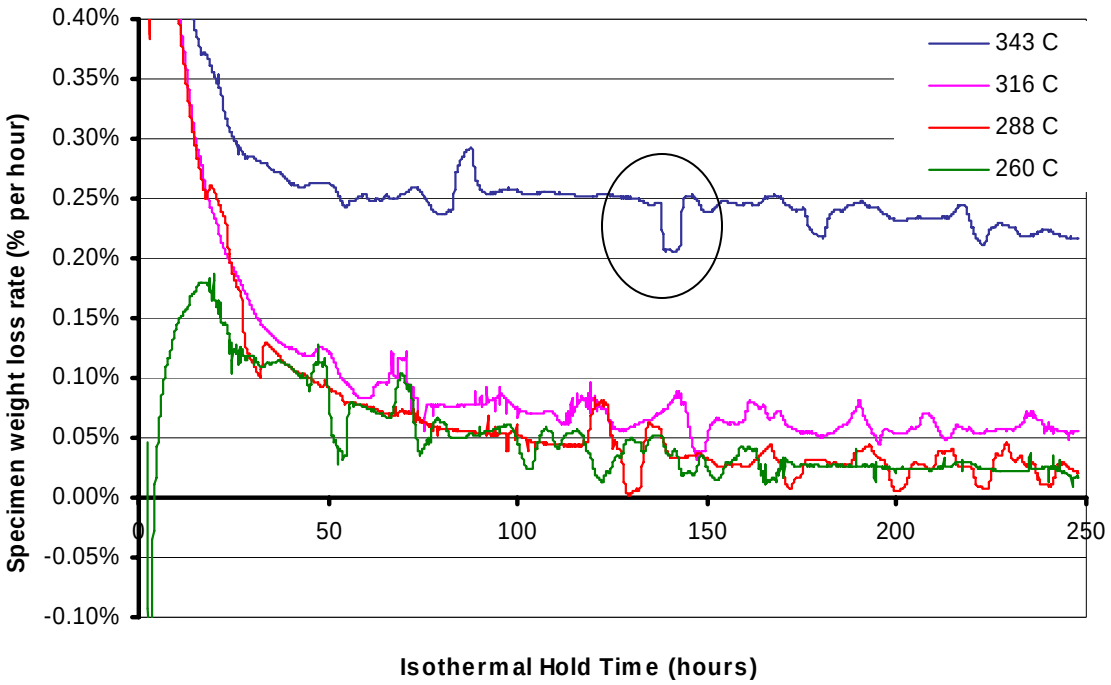

Figure 22: Rate of Normalized Weight Loss in Air

From inspection, even at 343 °C, an exact constant rate of weight loss is not reached. However, when the rate between 50 hours and 250 hours is compared to the first 50 hours, the average rate varies little from the actual during the last 200 hours of testing. Through the same reasoning, the average loss rates can be approximated for the remaining temperatures and are summarized in Table 3. The transition point to the linear weight loss rates is more gradual for the three lower temperatures when compared to 343 °C.

The general results in air, identification of a steep initial rate of weight loss followed by a reduced rate of weight loss, is consistent with other TGA research that has been conducted on PMR-15. Bowles et al (8) and Bowles and Meyers (10) both found similar trends when testing neat resin plaques and composite panels respectively.

Low Temperature Weight Gain and Moisture Evaporation

Figure 23 presents the first 250 minutes of normalized weight for tests in air. The plots show a rapid drop of 1%-2%, a short constant normalized weight and then either a weight gain or drop depending on the test temperature. The initial drop was due to absorbed moisture content that evaporated off during the initial ramp up to 110 °C and the isothermal hold at 110 °C. The moisture hold time durations for each test and the normalized moisture content for each test are presented in Table 3. As soon as the temperature was ramped up to the test temperature following the moisture isotherm, all tests but the 343 °C test exhibited a short duration weight gain. The 260 °C test even exceeded its original recorded weight including the absorbed moisture. The weight gain decreased as the aging temperature increased and was entirely eclipsed by weight loss mechanisms in the 343 °C test. Initially, it was theorized that oxygen from the air was bonding to the polymer making it gain weight. However, as will be discussed later, a similar finite weight gain was also experienced in an inert environment containing no oxygen.

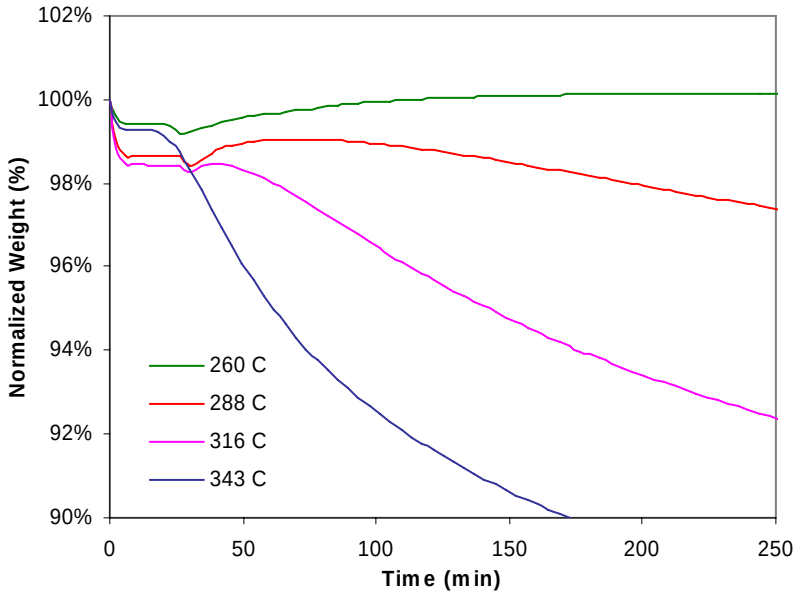

Figure 23: TGA of PMR-15 Neat Resin Powder in Air (0 to 250 min)

Time-Temperature Superposition Analysis

The principle of Time-Temperature Superposition was applied to the test results in air with success. Figure 24 presents the curves at 260, 288, and 316 °C shifted to 343 °C and Figure 25 is a plot of the log of the shift factors (A_t) versus the difference in the inverse master curve temperature and the test temperature as in Eq. (10).

The quality of fit shown in Figure 24 was not as good for early data in the test (0 to 200 min or up to 2.3 on the log scale) as the fit of data after that time. The poorer quality of fit is a result of the heavily temperature dependent initial rate of weight loss which may be attributed more to the diffusion of the reaction products remaining after curing and post-curing rather than from the weight loss associated with the environmental degradation products which is being modeled by the Arrhenius-type relation. Similarly, if the surface area was reduced quickly, as may have occurred if a large portion of smaller particles were present and completely degraded relatively quickly, then the quality of fit may also be affected early in the test.

The linear relationship shown in Figure 25 is based on subjectively shifting the plots in order to match the conclusion of the tests as opposed to the beginning. The linearity suggests that the weight loss of the neat resin powder can be modeled by the Arrhenius-type relation and thus extends the usefulness of the testing such that the weight loss at intermediate temperatures can be predicted. The equation for the line that best fits the shift factor data is shown on the plot for use in such a process.

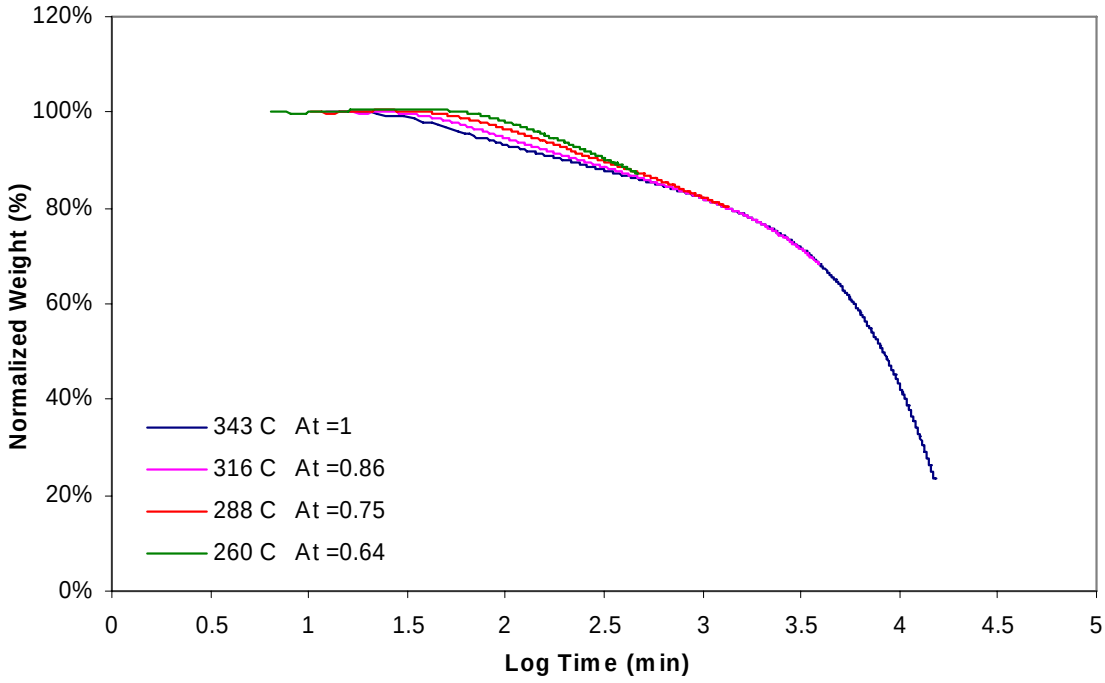

Figure 24: Time-Temperature Superposition of TGA Air Results (343 °C master curve)

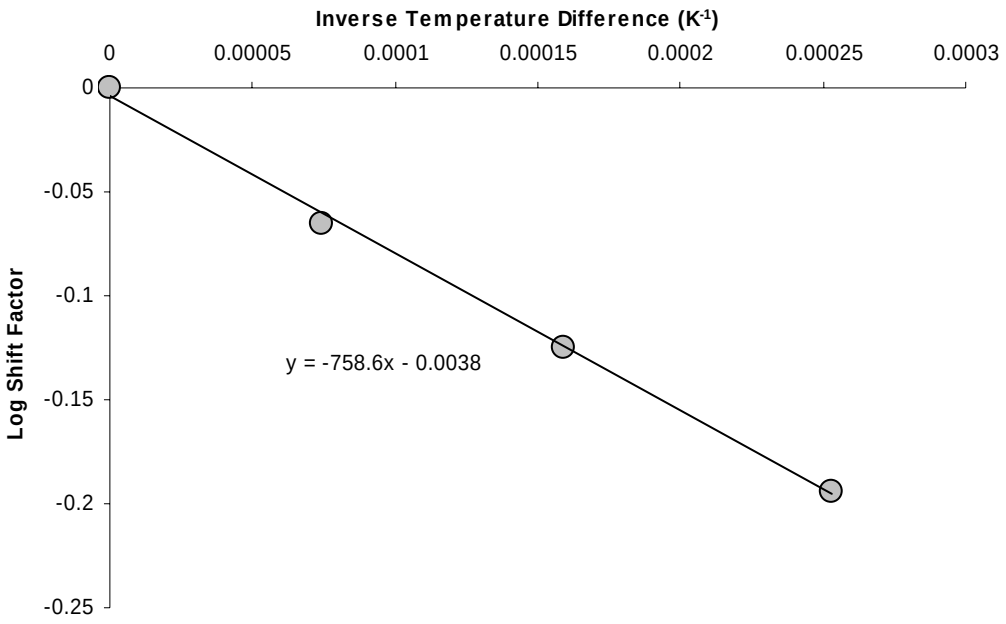

Figure 25: Time-Temperature Superposition Shift Factors for Air

TGA Results in Oxygen

General Trends

Thermo-gravimetric testing in oxygen at 288, 316 and 343 °C was completed and the results of the tests are summarized numerically in Table 4. The normalized weight as a function of aging time is presented graphically in Figure 26. The data for the 260 °C test found in Figure 26 is not actual TGA data, but rather predicted results based on the master curve created through the application of Time-Temperature Superposition which will be discussed in the *Time-Temperature Superposition Analysis* section. The results for 343 and 316 °C are re-tests after problems with the purge gas regulator arose during the first tests.

Table 4: Summarized Test Results in Oxygen

Test Temperature (°C)	288	316	343
Initial Weight (mg)	9.960	10.181	10.580
110 °C Hold Time (min)	15	13	12
Moisture Content (%)	0.8%	0.5%	0.4%
Final Weight (mg)	7.234	4.623	0.316
Final Normalized Weight (%)	72.63%	45.41%	2.99%
Linear Weight Loss Rate (%/hr)	0.038%	0.124%	N/A
Linearity Transition Time (hr)	160	120	N/A

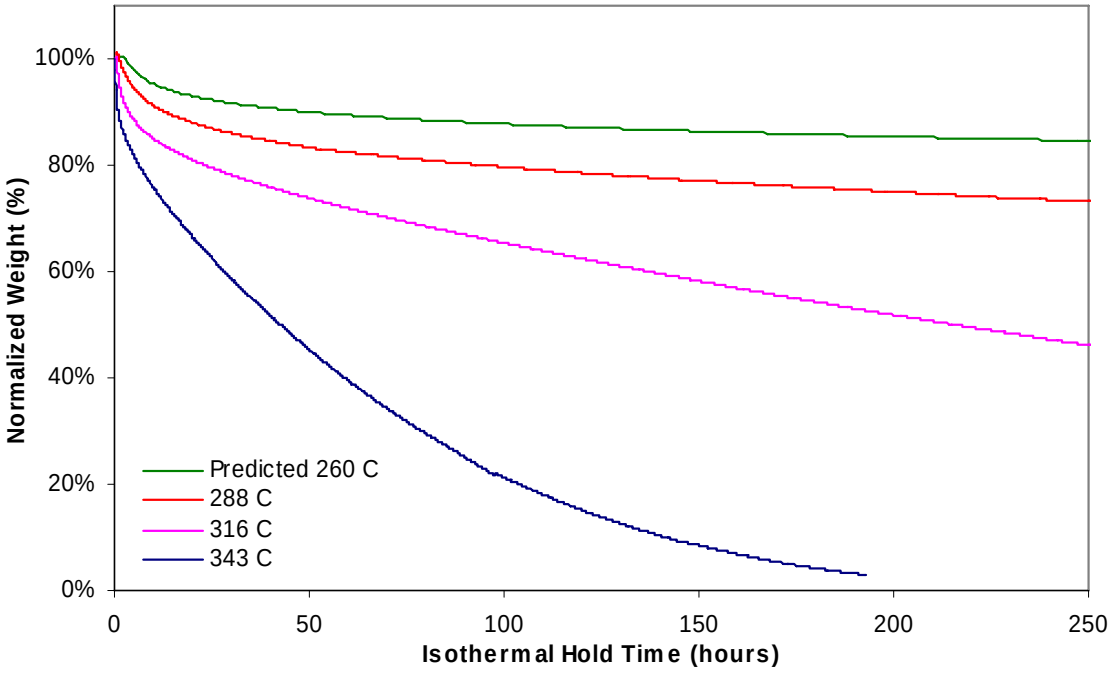

Figure 26: TGA of PMR-15 Neat Resin Powder in Oxygen

The results for 316 and 288 °C in oxygen exhibited the same trends as the specimens in air. There was a higher initial weight loss followed by a transition to a near constant rate of weight loss. The 343 °C test in oxygen started similarly, but never approached a constant rate of normalized weight loss. Its normalized weight dropped quickly then began to approach zero asymptotically. This process is best observed by plotting the rate of normalized weight loss per hour over the course of the test as shown in Figure 27. The specimen chemically degraded so quickly that the rate of degradation

became limited by the availability of polymer for reaction as opposed to settling on a degradation rate that was dependent on the aging temperature.

Figure 27 was also used to determine the linear weight loss transition times presented in Table 4. The process was the same that was used to determine the transition points in the air tests and thus were also approximations based on relative changes in the slope of the lines. The linear weight loss rates were different from air in more than just the actual values. The data used to calculate the rates of weight loss in oxygen contained much less noise than the air data. As a result, no running averages were necessary to smooth the data before interpretation could take place. The reduced noise was due to the use of a low-pressure, two-stage purge gas regulator that reduced the fluctuations in the gas flow. The purge gas for the air tests was house air and thus subject to any pressure fluctuations that occurred elsewhere in the system.

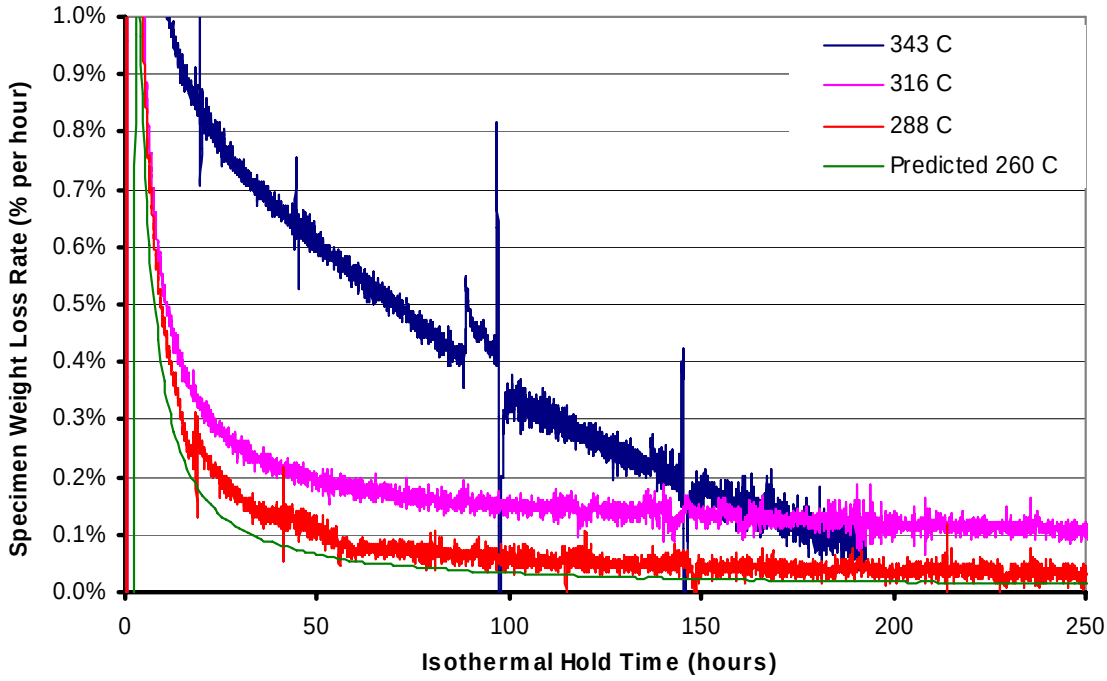

Figure 27: Normalized Rate of Weight loss in Oxygen

The 343 °C test also exhibited different behavior during the first 20 minutes of testing than was expected. After the 110 °C moisture hold was completed and the ramp up to 343 °C was initiated, the normalized weight dropped abruptly at a rate of 40 and then 78 % per hour and then immediately settled on a weight loss rate of 4 and then 8%. Figure 28 is a plot of the normalized weight and the furnace temperature plotted together for the first 1.5 hrs of testing. The uncharacteristic weight loss coincides precisely (within the range of a single data point) to the time during which the TGA ramped the temperature up to 343 °C. No other tests exhibited this extreme rate of weight loss during the ramp up to the test temperature. The next closest rate of weight loss observed during this research occurred during the first 5 minutes of testing when the moisture was evaporating out of the specimens. The highest rates experienced during this time for all of the other tests only ranged from 10 to 30 %. Explanations for this extremely high rate weight change may include partial combustion of the specimen or some kinetic activity that may have disturbed the specimen in the basket such as a small explosive event brought on by the rapid increase in temperature much like a kernel of popcorn bursting open displacing the surrounding kernels.

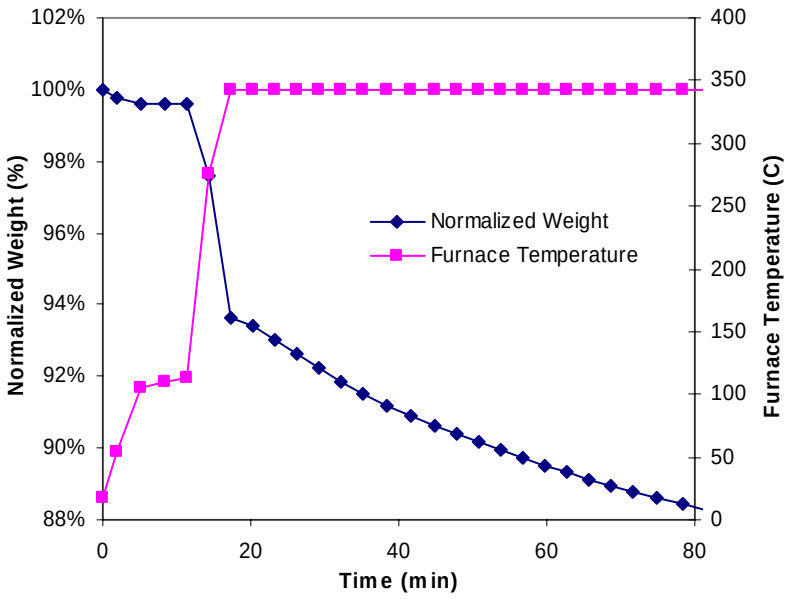

Figure 28: Rapid Rate of Weight Loss during 343 °C Test in Oxygen

Low Temperature Weight Gain and Moisture Evaporation

The moisture content and hold times for the oxygen tests can be found in Table 4 above. Figure 29 below shows the first 250 minutes of testing in oxygen. There are two major differences in the appearance of the data between the oxygen and the air environments: 1) the normalized weight for the 288 and 343 °C data does not appear to become constant with respect to time during the 110 °C moisture hold time; and 2) the lifetime of the weight gain mechanism in oxygen is shorter than the respective lifetime in air. The longer 110 °C moisture hold durations in air (23 minute average) were found to be unnecessary after review of the results because the constant normalized weight became steady in a period of time much shorter than what was allowed. Consequently, the moisture hold times in the oxygen tests were reduced. The data traces in Figure 29 give the appearance that the specimens were not allowed to reach a constant normalized value. The misrepresentation is due the compression of the TGA data as it was transferred from the TGA to the PC Software. The TGA sampled the data (furnace

temperature, specimen weight, and their associated time) at 30 second intervals and updated the real time plot on the PC Software at the same interval. This allowed the operator to observe the constant normalized weight reached after the moisture was evaporated. However, when the file was saved at the test conclusion, compression of the data file resulted in data points 4 minutes apart. The result was fewer data points that, when plotted with smooth lines, appear to gradually decrease then increase, never reaching a constant normalized weight when the test specimen had actually reached a constant weight.

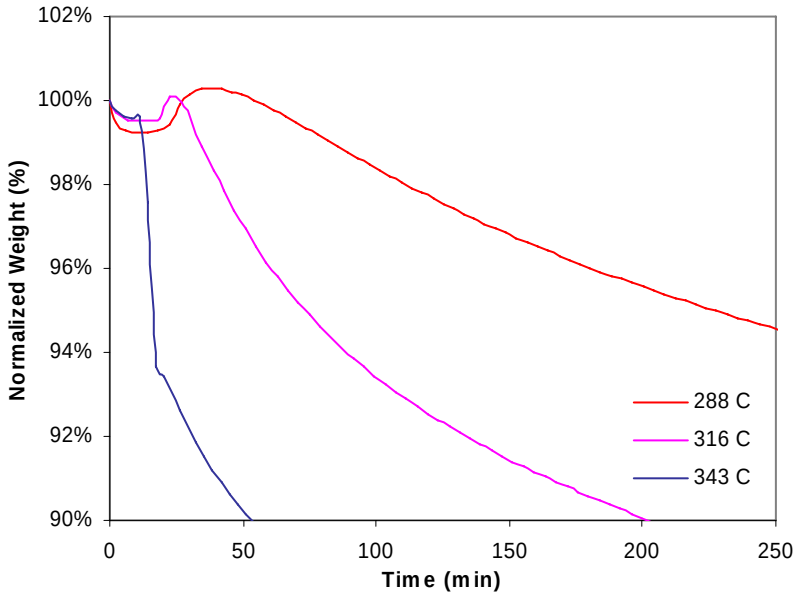

Figure 29: TGA of PMR-15 Neat Resin Powder in Oxygen (0 to 250 min)

The weight gain mechanism that manifested itself in all but the 343 °C air tests was also present in the pure oxygen environment. The difference was the duration of the gain phenomenon, roughly a factor of two. It is unclear whether the weight gain mechanism is truly shorter in duration or the weight loss mechanisms are occurring at a greater rate making the weight gain appear shorter.

Time-Temperature Superposition Analysis

Time-Temperature Superposition was applied with success for the tests in oxygen. The data was plotted similarly to air with the exception that the 316 °C test was used as the master curve. Again, when shifting the data, the focus was to align later portion of the data sets. The anomalous high weight loss event experienced by the second 343 °C test resulted in a poor fit of the data in the first 200 minutes of testing. It is unclear whether the 343 °C test would have aligned better with the master curve if this event had not occurred. A re-test would be needed to reach a conclusion. Figure 30 shows the master curve and the 288 and 343 °C data shifted to it. Figure 31 shows the plot of the log of the shift factor plotted verse the difference in the inverse master curve temperature and the test temperature as in Eq. (10). Similar to the air results, the relationship between the shift factor and the inverse of temperature is proportional as indicated by the linear relationship validating the assumption of an Arrhenius-type rate process.

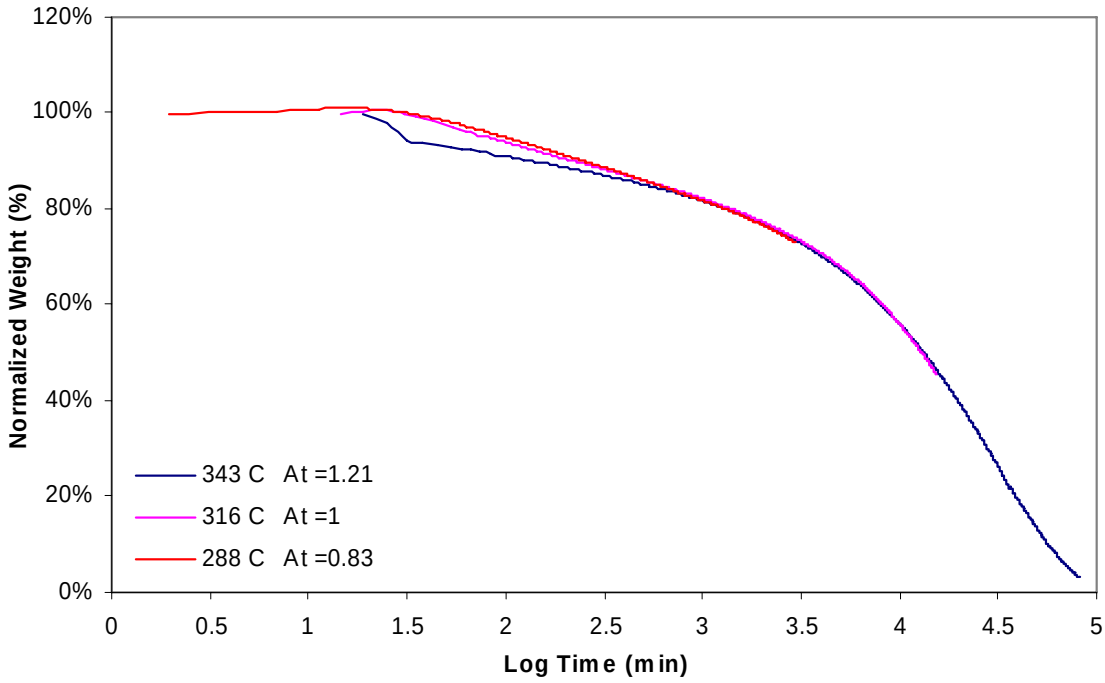

Figure 30: Time-Temperature Superposition of TGA Oxygen Results (316 °C master curve)

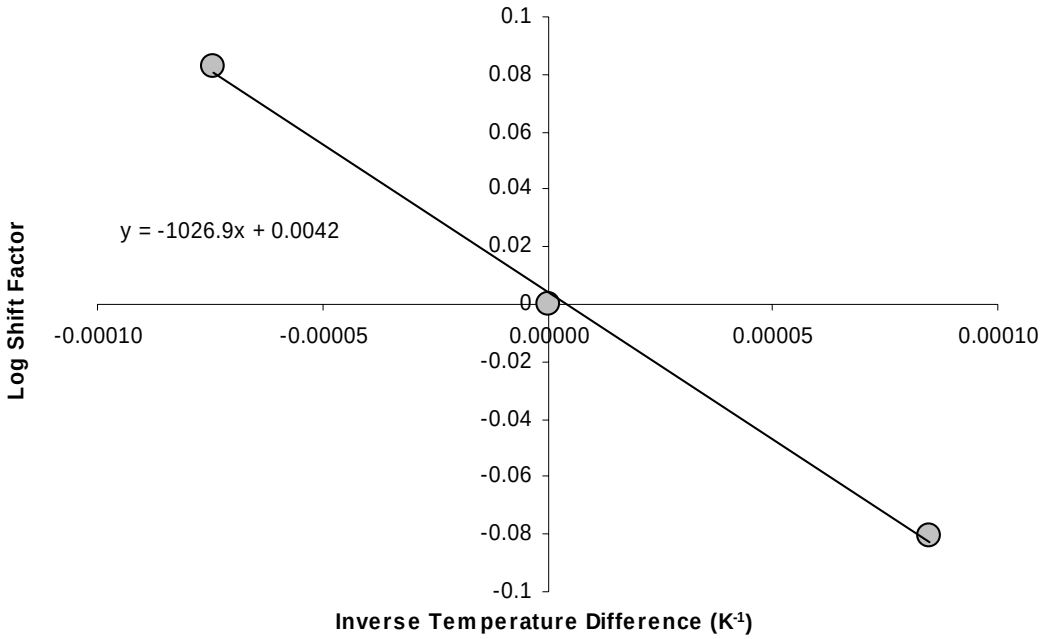

Figure 31: Time-Temperature Superposition Shift factors for Oxygen

There was not time to complete the 260 °C test in oxygen. However, the assumption of the Arrhenius-type relation was found to be appropriate and thus was used to predict the 260 °C data from the master curve. To do this, the process that was use to shift data to the master curve is reversed. Using the equation for the line presented in Figure 31 above, the shift factor for 260 °C was calculated to be 0.67. With this number, the new time points for 260 °C data were calculated by raising 10 to the ratio of the master curve time points divided by the shift factor as shown below in Eq. (11).

$$\text{Time}_{260} = 10^{\frac{\text{Time}_{\text{master}}}{A_t}} \tag{11}$$

Using Microsoft® Office Excel the data the shift was propagated through the master curve time data to yield the shifted time value and was associated with the corresponding original normalized weight measurement from the master curve (316 °C normalized weight data) and plotted. The results were shown above in Figure 26 as "Predicted 260 C".

Experimental Complications

Burn up of the first 343 °C test

The results for the first test in oxygen at 343 °C are shown in Figure 32. In order to assist in interpretation, a plot of the furnace temperature was overlaid with the normalized weight. The test started normally proceeding through the moisture hold time after which the heating program was ramped up to the test temperature. As the temperature ramped up, the normalized weight began to drop. When the temperature reached 300 °C 12.5 min into the test, the normalized weight dropped very abruptly: from 0.988 to 0.066. Concurrently, the furnace temperature rose to 385 °C in same 1.5 minutes of the test. The large, abrupt weight change and the 42 °C temperature overshoot suggested that the sample had combusted in the high temperature oxygen. The lab supervisor noted the anomalous output and stopped the test at the 48 minute mark. A visual inspection of the specimen upon removal from the furnace confirmed the combustion theory, as only small amount of black char was present in the platinum basket.

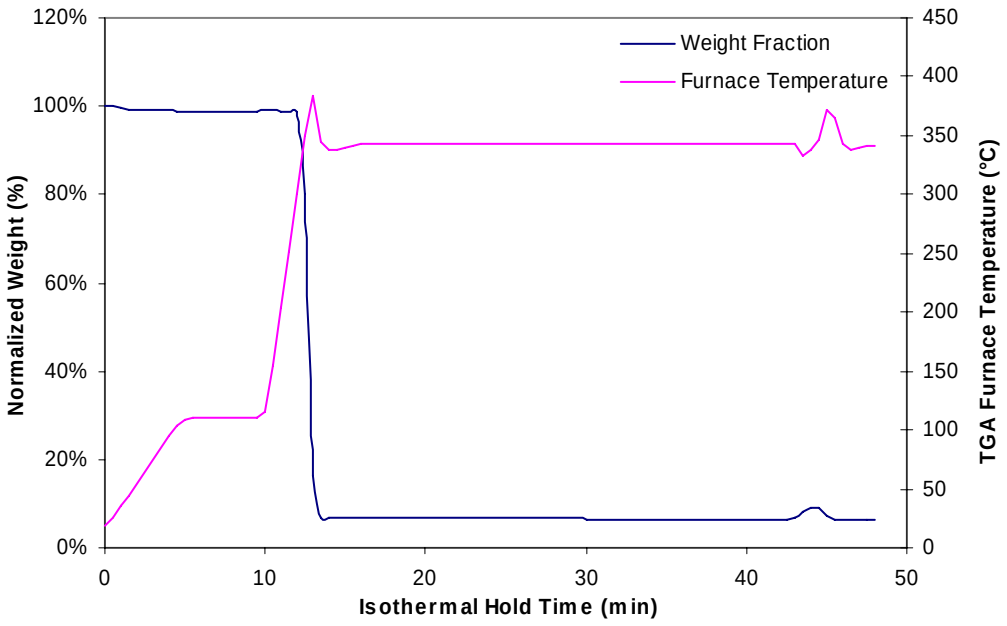

Figure 32: TGA of PMR-15 Neat Resin Powder in Oxygen at 343 °C (Trial 1)

Regulator issues for 316 and 288 °C tests

The Oxygen testing was postponed after encountering problems during the 316 °C test and the 288 °C test. The first test at 316 °C was not used in this thesis because the supply of oxygen purge gas dropped to zero during the test slightly affecting the rate of weight loss experienced by the specimen. The problem arose slowly and was discovered on day 5 of testing. Adjustments to the flowmeter or the regulator could not be made to correct the dropping purge gas flow as any pressure variations created would have been felt by the balance and corrupted the data. The lab supervisor was unavailable, so the decision was made to allow the test to complete in lieu of stopping prematurely. The test results are shown in Figure 33 and are presented along side the successful 316 °C test.

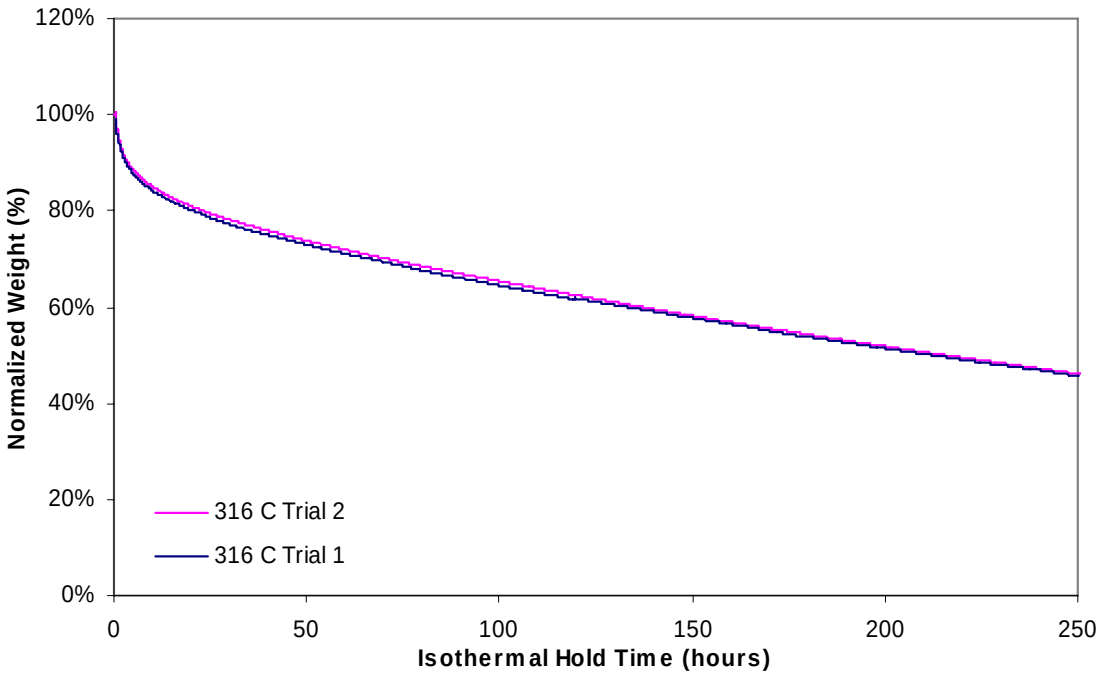

Figure 33: Comparison the TGA retest of PMR-15 Neat Resin Powder in Oxygen at 316 °C

The problem and results were discussed after the test conclusion with the project sponsor and it was agreed that the test should be performed again if time allowed after the remaining testing had been completed. The process of lining up the purge gas system was also changed. It was decided that all of the tests utilizing bottled gas and a pressure regulator should be run at a higher output pressure of 10 psi as opposed to 5 psi in an effort to operate the regulator farther from the end of its controllable range, 0 psi. It was also decided that the purge gas flowmeter should be adjusted and allowed to equalize overnight. The next day the flowmeter would be readjusted prior to starting the test.

Oxygen testing continued with the setup of the 288 °C test until the oxygen regulator completely failed to operate during test preparations. Investigation revealed that internal components were sticking and preventing smooth actuation that is required for precise pressure control. At this point, a new two-stage low pressure regulator was ordered through AFRL channels in an effort to avoid any future purge gas problems.

However, problems with delivery delayed further oxygen testing. Two-day shipment was promised, however it took three weeks to arrive. In the mean time, the 343 °C test in argon was performed. The two-stage regulator finally arrived and Oxygen testing was started over yielding the results presented in the thesis results chapter.

TGA Results in Argon

General Trends

Thermo-gravimetric analyses at 288, 316, and 343 °C in argon were completed and their results are summarized in Table 5 and the normalized weight as a function of time shown in Figure 34. Time constraints prevented the completion of a test at 260 °C.

Table 5: Summarized Test Results in Argon

Test Temperature (°C)	288	316	343
Initial Weight (mg)	10.057	10.726	10.222
110 °C Hold Time (min)	19	24	26
Moisture Content (%)	0.5%	0.8%	0.5%
Final Weight (mg)	9.177	10.093	8.869
Final Normalized Weight (%)	91.25%	94.10%	86.76%
Linear Weight Loss Rate (%/hr)	0.0019%	0.0069%	0.0099%
Linearity Transition Time (hr)	210	200	100

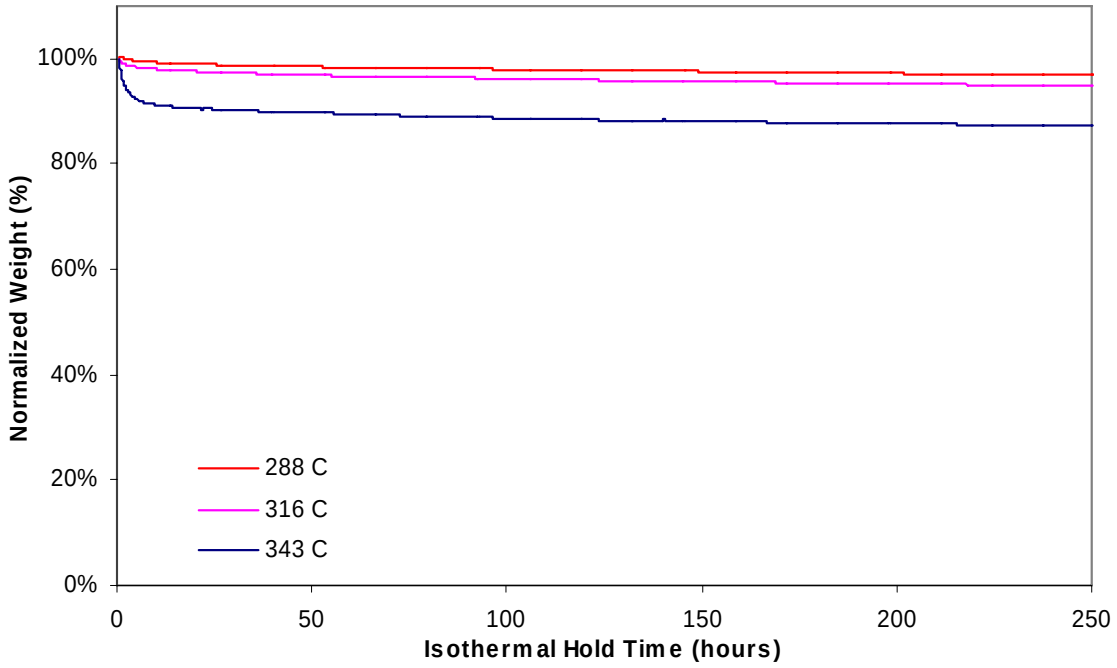

Figure 34: TGA of PMR-15 Neat Resin Powder in Argon

The trends present in Figure 34 are qualitatively similar to those observed in testing in air and oxygen. The rate of normalized weight dropped the fastest in the beginning of the test and then transitioned to a slower, relatively constant rate of weight loss thereafter. The initial rate of weight loss was heavily temperature dependent. The difference between the 343 °C data and the 316 and 288 °C data appears unproportionally large especially during the initial high rate of weight loss when compared to the differences found in oxygen and air between the same temperatures. This highly temperature dependent rate greatly separated the 343 °C data from the 316 and 288 °C data. Conversely, the near constant rates arrived at for the 316 and 343 °C test were very close, thus suggesting that the linear weight loss rates due to long term volume aging are not as temperature dependent as the initial rates of weight loss. Figure 35, a plot of the rate of normalized weight loss in percent per hour as a function of time, was used to determine the transition point to the linear rates of weight loss. The data used to make the

plot was a running average over a 5 hour period in order to remove noise and improve clarity and presentation. The method is the same that was applied to the air data. The oscillatory pattern will be addressed below in *Experimental Complications*. Despite the oscillation, the transition points were identified and are shown in Table 5 above. The rates of normalized weight loss per hour are the averages over the respective linear ranges.

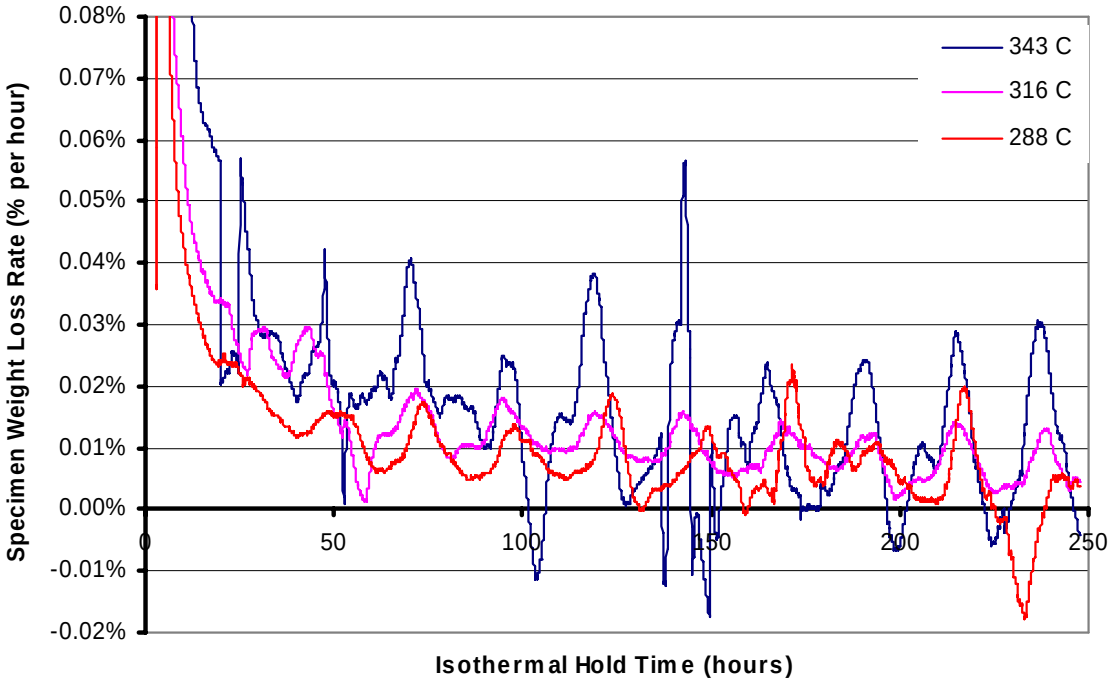

Figure 35: Normalized Rate of Weight Loss in Argon

Lower Temperature Weight Gain and Moisture Evaporation

The normalized weight during the first 250 minutes of the argon tests can found in Figure 36. The moisture evaporation and the 110 °C moisture hold are clearly seen because the hold time had been increased after the oxygen tests. The results and details can be found in the argon test summary, Table 5 above.

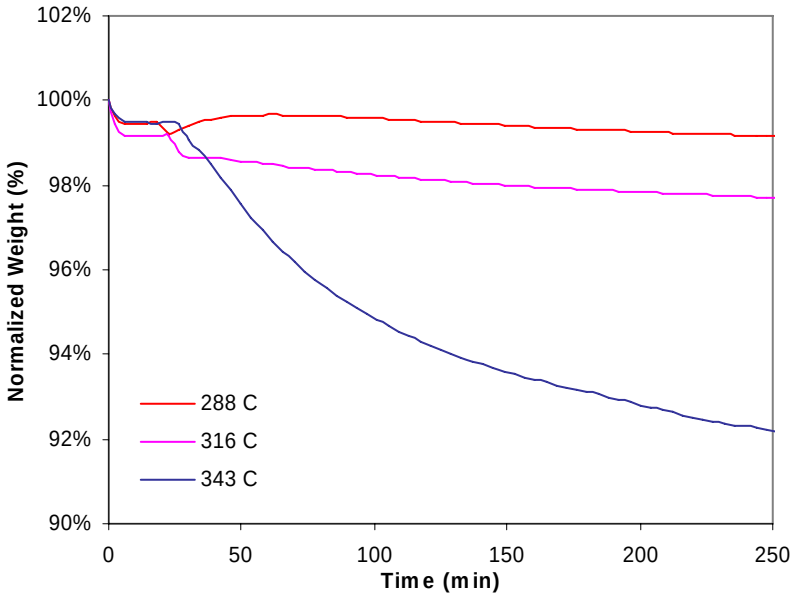

Figure 36: TGA of PMR-15 Neat Resin Powder in Argon (0 to 250 min)

Following the 110 °C moisture hold, the 316 and 343 °C tests proceeded into a high rate of weight loss that had been typical for this thesis. The results of the 288 °C test were different in that the specimen experienced a weight gain similar to that of the other environments. It had a finite lifetime that ended either due to the fading of the mechanism that drove the weight gain or masking of the mechanism by larger weight loss mechanisms.

Time-Temperature Superposition Analysis

The principle of Time-Temperature Superposition was not successful for the test results in argon. Figure 37 presents the 288 and 316 °C data shifted along the log time scale to the 343 °C data and Figure 38 plots the log of the shift factors verse the differences in the inverse master curve temperature and the test temperature as in Eq (10). The three traces did not align in Figure 37 due to the large differences in the initial rate of weight loss. However, when the normalized weight data for 288 and 316 °C was shifted down uniformly (subtracting the same factor (V) from each normalized weight data

point), then the curves did align after the initial stages of testing (800 minutes or 2.9 on the log time scale). The results of the combined shifting are presented in Figure 39. It should be noted that the vertical shift technique used does not have theoretical basis tantamount to the time shifting. This technique essentially had the effect of removing the highly temperature dependent initial weight loss that was observed in argon. Regardless of the vertical shift, the time shift factors (A_t) did not conform to a linear relationship with the inverse temperature differences as shown in Figure 38. The lack of linearity suggests that long-term rate of weight loss attributed to volume aging may be less temperature dependent than long-term linear thermo-oxidative weight loss rates.

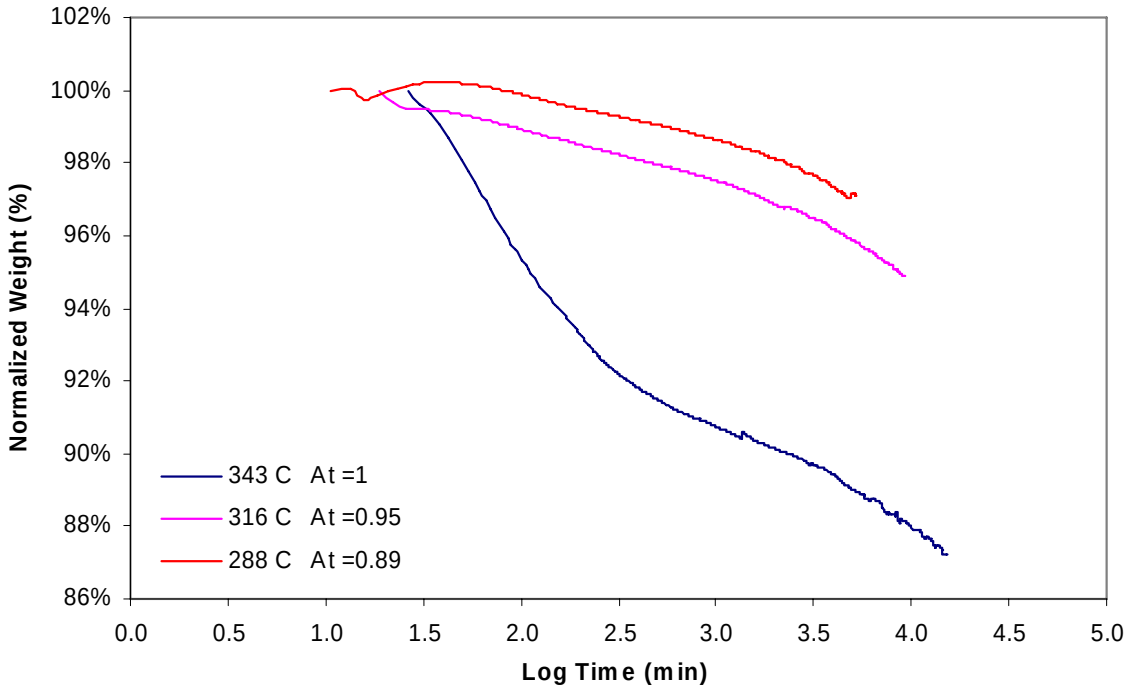

Figure 37: Time-Temperature Superposition of TGA Results in Argon (343 °C master curve)

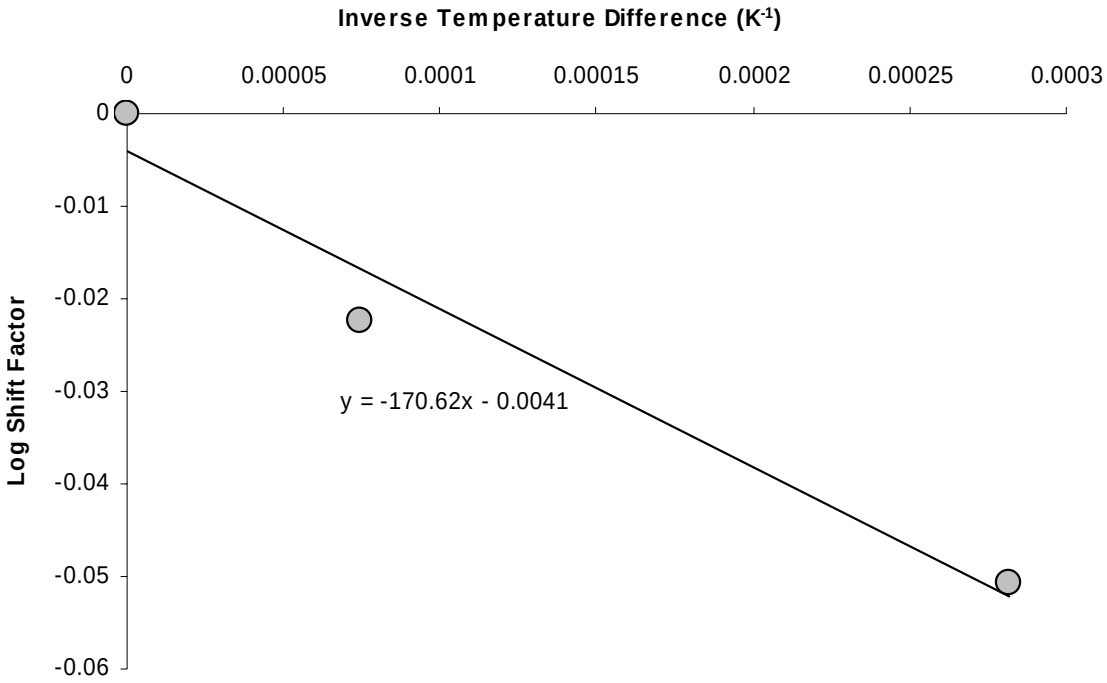

Figure 38: Time-Temperature Superposition Shift Factors for Argon

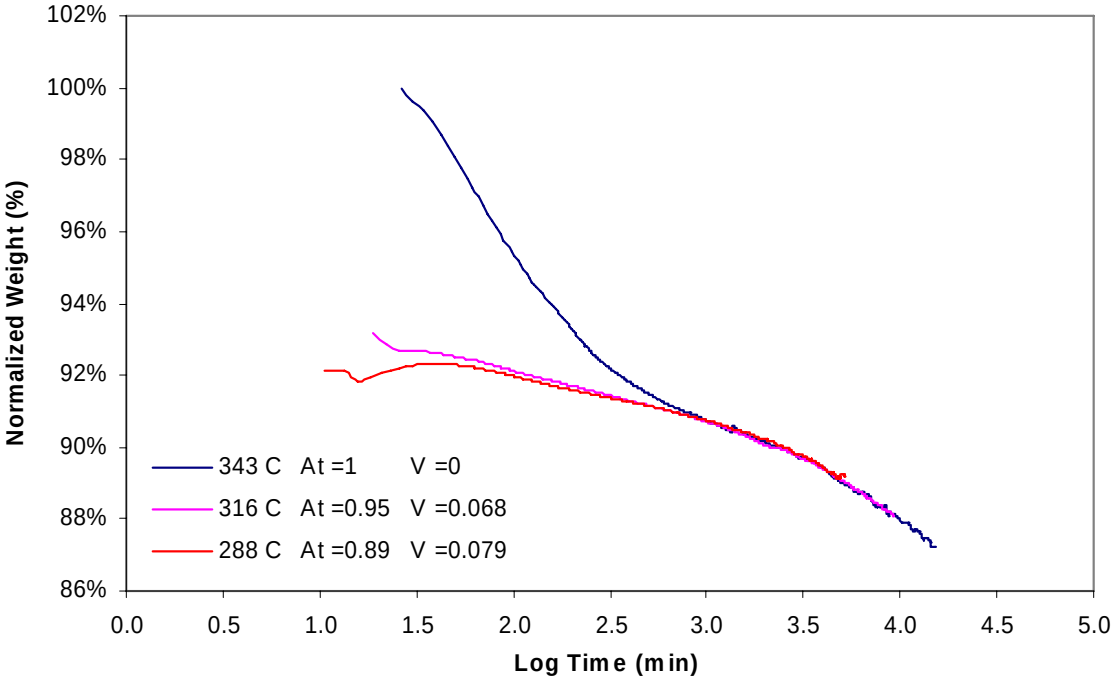

Figure 39: Vertical and Horizontal shifting of TGA results in Argon (343 °C master curve)

Experimental Complications

The tests in argon were successful, but there were problems with the quality of the data. As mentioned above, oscillations were observed in the data. In Figure 34 above, the normalized weight curves appear smooth. However, if only the linear weight loss region is presented alone as in Figure 40 below, the oscillatory trend that was first observed in Figure 35 can easily be seen. Two possible causes included: 1) daily fluctuation in the building's ventilation system or 2) purge gas regulator fluctuation. The period of the oscillations was found to be roughly 24 hours and thus initially theorized to be related to some daily event that affected the atmospheric pressure in the building where the tests were conducted. However, determination of the actual times during the day when peaks and troughs occurred proved to be inconsistent between the three tests.

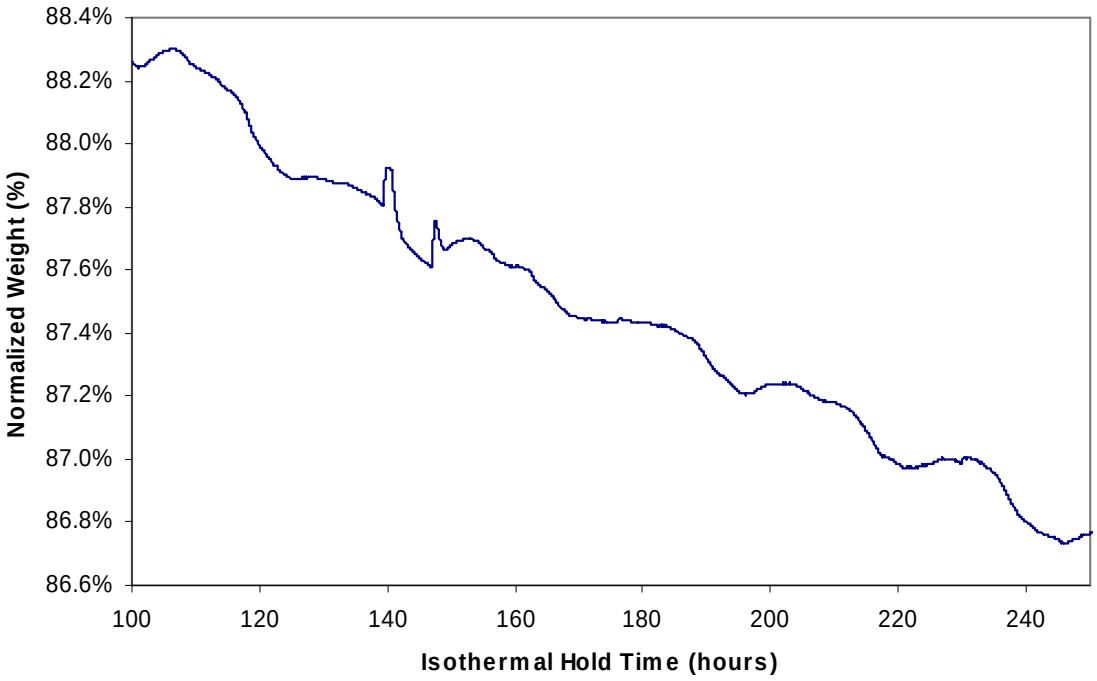

Figure 40: TGA of PMR-15 Neat Resin Powder Aged at 343 °C in Argon (100 to 250 hrs)

It was then agreed that the fluctuations were attributed to the argon purge gas pressure regulator. The valve in the regulator automatically adjusts itself to provide the

same outlet pressure regardless of the inlet pressure. As tests progressed, the amount of gas in the bottles was constantly decreasing therefore reducing the inlet pressure to the regulator (a drop of 300 psi during the 250 hours of testing was common). The valve adjusted itself and this adjustment was thought to be the source of the oscillations. This phenomenon was limited to the argon regulator because the new two-stage low-pressure oxygen regulator did not exhibit the same behavior when the data was examined on a similar scale. If further testing is conducted, funds should be invested in new low-pressure regulators for use with the TA Instruments TGA when utilizing bottled purge gases.

Comparison of TGA Results Between Aging Environments

The TGA results for 343, 316, and 288 °C for all the gaseous environments are presented in Figure 41, Figure 42, and Figure 43 respectively. These figures illustrate that the weight loss of PMR-15 neat resin powder at similar temperatures was much greater in environments with higher concentrations of oxygen. When operating under the assumption that volume aging weight loss and thermo-oxidative weight loss are decoupled, the relative weight loss attributed to a particular condition can be readily viewed as well. At temperatures of 316 °C and below the effects of volume aging on weight loss are negligible when compared to the weight loss that can be attributed to thermo-oxidation. Abdeljaoued (19) expanded upon this idea testing PMR-15 in 4 different partial pressures of oxygen. The results were qualitatively similar.

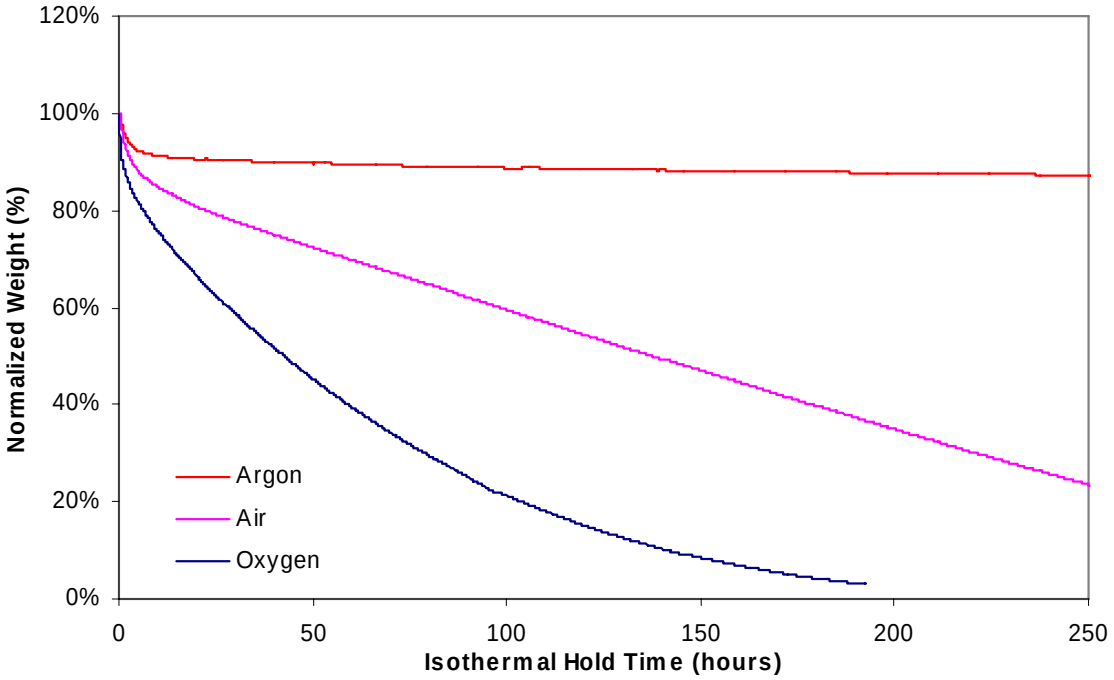

Figure 41: Comparison of TGA of PMR-15 Neat Resin Powder at 343 °C in Oxygen, Air, and Argon

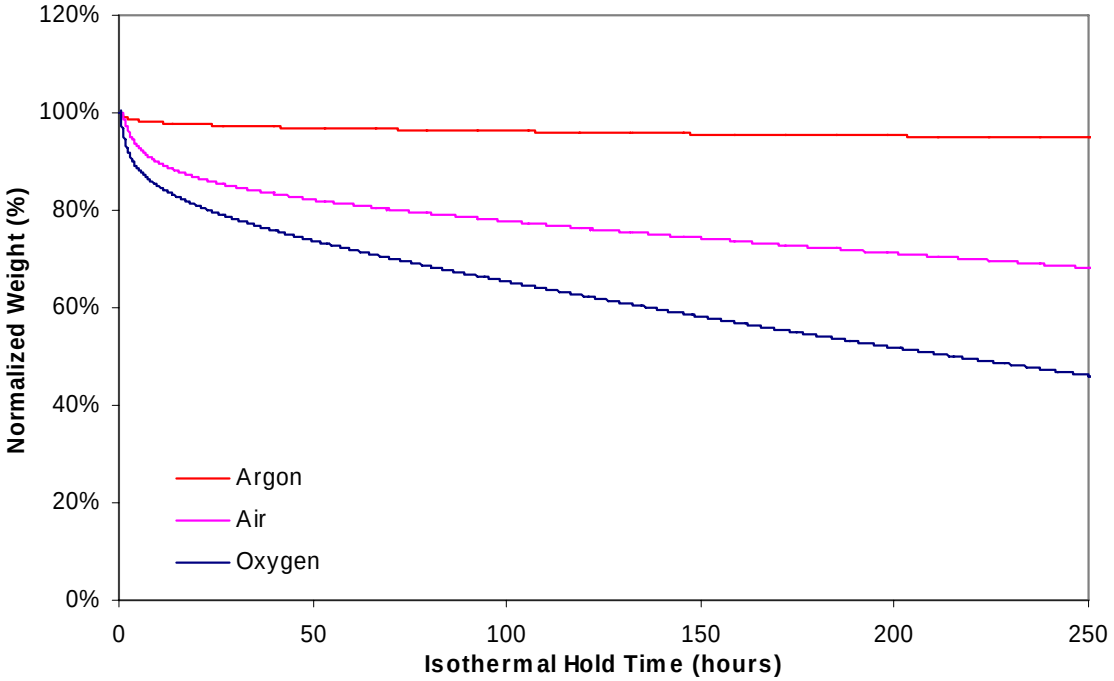

Figure 42: Comparison of TGA of PMR-15 Neat Resin Powder at 316 °C in Oxygen, Air, and Argon

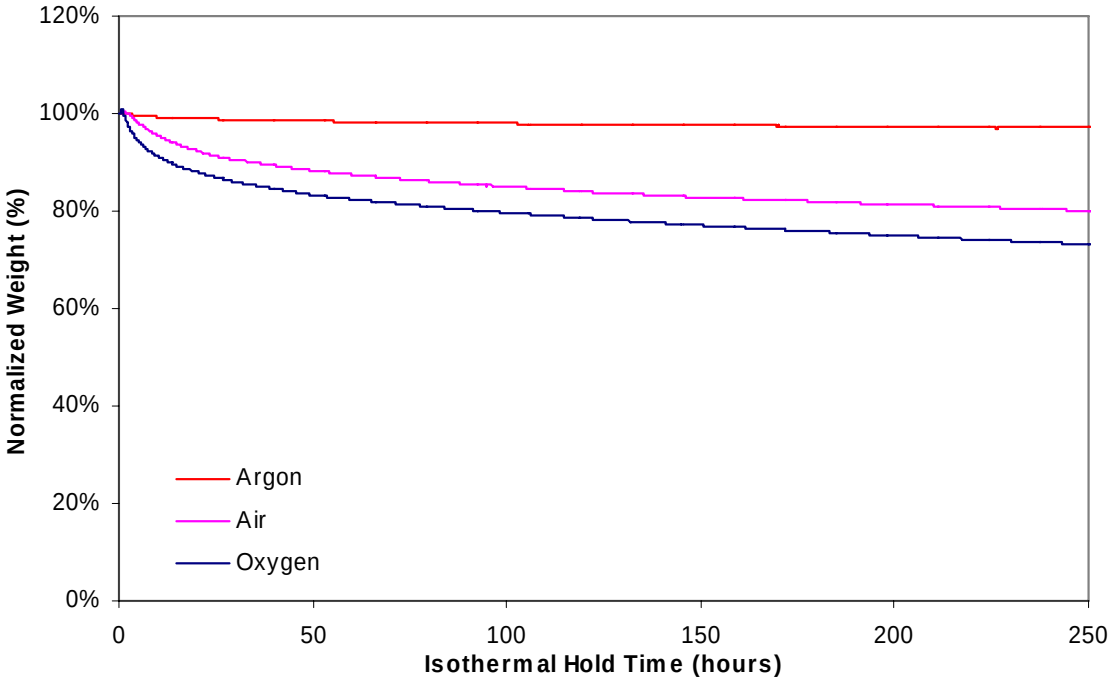

Figure 43: Comparison of TGA of PMR-15 Neat Resin Powder at 288 °C in Oxygen, Air, and Argon

AFRL/Materials Directorate Thermo-Oxidation Layer Modeling Parameters

Concentration Dependence Model: β Parameters

The normalized concentration parameters, βC, used in the reaction rate reduction model presented in Eq. (4) and repeated below were solved using the data from the air and oxygen tests. Because the weight loss is assumed to be proportional to the oxygen consumption rate, the ratio of the weight loss at two concentrations is the same as $R_1(C_1)/R_2(C_2)$. Thus,

$$\frac{2\beta C_1}{1+\beta C_1}\left[1-\frac{\beta C_1}{2(1+\beta C_1)}\right]=\left(\frac{\text{Weight loss Air}}{\text{Weight loss } O_2}\right)\frac{2\beta C_2}{1+\beta C_2}\left[1-\frac{\beta C_2}{2(1+\beta C_2)}\right] \qquad (12)$$

The C_1 is the concentration of oxygen in air, 0.79 mol/ m^3 and C_2 is the concentration of pure oxygen, 3.74 mol/m^3. The ratio of normalized weight loss between oxygen and air are shown in Figure 44. For 288 and 316 °C the average ratio for the last 160 hours was used. These points correspond to the points were the ratio reaches a relatively constant

value with respect to the range of the data from start to finish. The limits of the averages also fall within the periods of time when the rates of normalized weight loss are considered constant. The ratio used for 343 °C was an average from the start of the linear range in air, 50 hrs, to the end of the oxygen test at 190 hours. The weight loss ratio for 343 °C has much greater variability than the other temperatures. The standard deviation is 0.05, while the standard deviation for 288 and 316 °C are 0.002 and 0.006, respectively. This spread in the data is due to the fact that the 343 °C oxygen test never reached a constant weight loss rate and the data used to calculate the ratios for plotting had to be manually extracted from plots of the normalized weight fractions. The manual extraction was necessary because, unlike the 288 and 316 °C tests, the time between each weight measurement was different due to the data compression that was explained in the *Oxygen Low Temperature Weight Gain and Moisture Evaporation* Section.

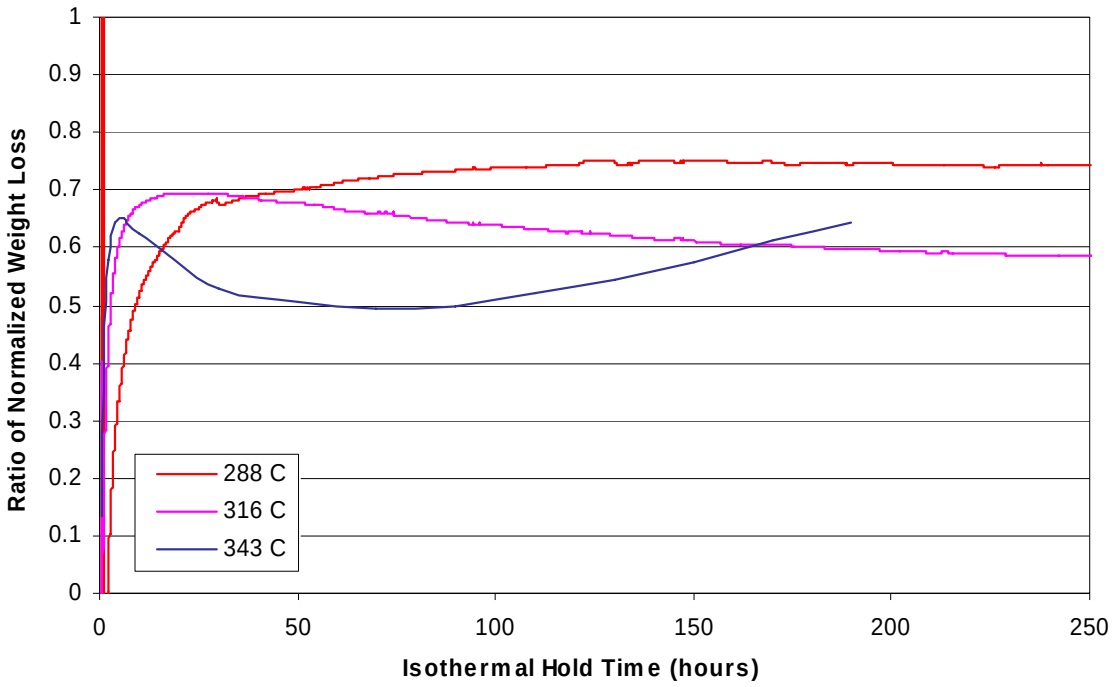

Figure 44: Ratio of Normalized Weight Loss between Air and Oxygen

Mathcad™ was used to solve the equation for the roots. The worksheet used for this step can be found in Appendix B. The solution yields three non-trivial roots, only one of which, the positive number, is a physically feasible result. The β parameters for the three tested temperatures are presented below in Table 6.

Table 6: Summary of Concentration Dependence Parameters

Test Temperature (°C)	288	316	343
Average Weight loss Ratio	0.745	0.594	0.549
Standard Deviation	0.002	0.006	0.052
β Value	1.114	0.594	0.491
Pochiraju and Tandon β Value	0.92 for 250 to 300 °C		

Saturation Reaction Rate Determination and Comparison

The saturation reaction rate (R_0) was calculated using Mathcad™ for the tested temperatures in air using Eq. (9) and the results are summarized in Table 7. The scaling constant (R_0*) and the activation constant (R_a) were provided by G. P. Tandon of the Air Force Research Laboratory Material's Directorate. The Mathcad™ worksheet used for calculation can be found in Appendix C.

Table 7: Summary of Saturation Reaction Rate Parameters for Air

Test Temperature (°C)	288	316	343
Activation Constant (J/mol)	23379.63	23379.63	23379.63
Scaling Constant (mol/m^3 min)	536.94	536.94	536.94
Saturation Reaction Rate (mol/m^3 min)	3.574	4.535	5.591
Pochiraju and Tandon Model R_0	3.5	N/A	5.5

Proportionality Constant Determination and Comparison

The proportionality constants (α) for 288, 316, and 343 °C were calculated using Mathcad™ and the results are shown below in Table 8. The summary table also presents the proportionality constants that were used in the Pochiraju and Tandon model for comparison.

Table 8: Summary of Proportionality Constant Parameters

Test Temperature (°C)	288	316	343
Reduction Concentration Function f(c)	0.717	0.537	0.483
Molecular Weight PMR-15 (g/mol)	1500	same	same
PMR-15 Measured density (g/cc)	1.3	same	same
α Value	0.00142	0.00321	0.01200
Pochiraju and Tandon Model Long term α Value	0.1	N/A	0.1

The proportionality constant (α) was calculated using the proposed relationship between the weight loss rate and the consumptive reaction term R(C) repeated below as Eq. (13).

$$\frac{dW}{dt} = \alpha R(C) \tag{13}$$

Solving Eq. (13) for the proportionality constant (α) and substituting in Eq. (3) and subsequently Eq. (4) and (5) yielded the expression (Eq. (14)) that was used to determine the values of α presented in Table 8.

$$\alpha = \frac{\left(\frac{dW}{dt}_{\text{air}} - \frac{dW}{dt}_{\text{argon}} \right) \rho_{unoxidized}}{R_0 f(C) \overline{M}} \tag{14}$$

The weight loss rate term expressed in Eq. (13) is meant to represent the weight loss rate attributed to thermo-oxidation alone. This rate was calculated by subtracting the weight loss rate in argon (assumed to be volume aging only) from the weight loss rate in air (assumed to be the sum of the thermo-oxidative weight loss and volume aging weight loss). This process is visible in Eq. (14). The rates were extracted from Table 3 and Table 5 and represent the long-term linear rates of weight loss.

The concentration dependence model (Eq. (4)) was evaluated with the concentration of oxygen in air, C_1=0.79 mol/m^{3}min and the β values presented in Table

6. The density (ρ) of unoxidized PMR-15 came from Schoeppner and Tandon (20) and the molecular weight was given as 1500 g/mol by the chemical formula for PMR-15. The Mathcad™ worksheet used to perform the calculations can be found in Appendix C.

The equivalent proportionality constants calculated differ significantly from the values used in the Pochiraju and Tandon model. The results were different due to the fact that the PMR-15 neat resin powder exhibited very different weight loss relationships from similar bulk material aging tests. It should be noted that the calculated proportionality constants (α) are constant because only the constant linear weight loss rates were used in the calculation of the β parameters and the proportionality constants (α). The Pochiraju and Tandon model varied the proportionality constant (α) linearly with time from 0.3 to 0.1 for the first 40 hours, and then fixed it at 0.1 thereafter. This decision was based on the qualitative trends exhibited by weight loss experiments reported by Ripberger et al (6) where the initial rate of loss was observed to be greatest and then decline with aging time to a constant. The theory was re-enforced by the improved simulation results that followed. A further extension of this thesis could include the derivation of an expression that could express the proportionality constant as a function of time for a given environment. A similar process could be pursued for the concentration dependence model, Eq. (4).

IV. Conclusions

Weight Loss in PMR-15 Neat Resin Powder

This thesis investigated the thermal and oxidative degradation of PMR-15 neat resin powder through the use of thermal gravimetric analysis (TGA) in air, oxygen, and argon air at isothermal hold temperatures of 260, 288, 316, and 343 °C for 250 hours. The TGA characterized the degradation by recording the change in neat resin powder mass versus time.

The qualitative results were similar for all tests. The specimens initially lost weight at a temperature dependent rapid rate followed by a reduction in the weight loss rate to a near constant value that was also dependent upon the isothermal temperature. The aging time corresponding to the start of the near constant rate of weight loss was also highly temperature dependent ranging from 50 hours at 343 °C in air to 210 hours at 288 °C in argon. The constant rates of weight loss increased with the concentration of oxygen and temperature of the aging environment. The test results in argon indicated that the degradation that occurred in the absence of oxygen (volume aging) was less temperature dependent than degradation that occurred in the presence of oxygen (thermo-oxidative aging). This conclusion is based on the comparatively small differences between the linear weight loss rates in argon as compared to differences between the tested temperatures in oxygen and air.

PMR-15 was found to experience a small weight gain phenomenon at 260, 288, and 316 °C in air and at 288 °C in argon. The phenomenon has a limited lifetime and magnitude that is temperature dependent. The effect is greatest at lower temperatures and

reduces in magnitude and duration as the aging temperature is increased. It is unclear whether the phenomenon is no longer occurring at higher temperatures or it is being masked by the temperature dependent weight loss.

Time-Temperature Superposition Application

Time-Temperature Superposition was evaluated as a method to extend the usefulness of the TGA test results. The assumed Arrhenius-type relationship for saturation reaction rates and their assumed proportional relationship to weight loss was validated for the tested temperatures in air and oxygen. It should be noted that these relationships are not a substitute of the application of molecular chemistry principles and the knowledge of the exact nature of oxidative reactions. However, in the absence of the precise quantum mechanics that drives the chemical changes, the representative relations are satisfactory and practical.

Parameters for Refinement of Air Force Research Laboratory Materials and Manufacturing Directorate Modeling Effort

The data from these tests will be used by researchers in the Air Force Research Laboratory Materials and Manufacturing Directorate to further efforts made towards developing a constitutive law and the associated models to predict the behavior of neat resin reinforced composites. The equivalent parameters used in the Pochiraju and Tandon model have been calculated and compared to those used in the model. The results were significantly different due to the fact that the PMR-15 neat resin powder exhibits very different weight loss relationships from bulk material aging tests.

Recommendations

This research was unique in that it was one of the first to perform weight loss measurements utilizing powdered polymer resin. The goal of powder experimentation was to remove the potentially limiting effect that oxygen diffusion may have on the rate of weight loss in PMR-15 neat resin. However, the results of this thesis cannot conclusively prove whether diffusion was a limiting factor. A conclusion may be reached by testing powdered resins of various particles sizes. By comparing the rates of weight loss as a function of particles size, it may be possible to identify a transition point in particle size when diffusion no longer significantly limits the thermo-oxidative weight loss.

It is also recommended that further research might include microscopic analysis or even scanning electron microscopy of powdered resin specimens during or after future thermo-gravimetric tests so that the state of oxidation may be visually identified. In this thesis the particle size ranged between 45 μm to 90 μm and did contain smaller particles that were not sifted out in the powdering process. It can be seen in Figure 2 that the oxidized surface layer reached a thickness of 96.4 μm after 196 hours at 343 °C in air. This layer thickness reported by Ripberger et al (6) was greater than the largest particle diameter found in the PMR-15 powder. This means that the weight loss occurring during the higher temperature tests may have transitioned from one characterized by PMR-15 oxidation to one characterized by the mass loss of completely oxidized PMR-15. Optical analyses may help determine if this transition is actually occurring.

If it was determined that the weight loss was associated with mass loss from completely oxidized PMR-15, the data could still be potentially useful to the AFRL/

Materials and Manufacturing Directorate's modeling effort. The Pochiraju and Tandon model currently assume that the oxidized material becomes chemically static after it reaches a specified state of weight loss defined by (ϕ_{ox}). If data from powdered resin weight loss experiments was found to be associated with mass loss from the oxidized PMR-15, then equations describing the mass loss could be added to build a more sophisticated model.

In addition to the aforementioned recommendations for future testing, the following recommendations are made to improve the quality of the experimental procedure and maximize the future application of the type of thermo-gravimetric testing outlined in this thesis.

1. The 260 °C tests in argon and oxygen should be performed to complete the PMR-15 Test Matrix presented in Table 1.
2. New low-pressure, high quality gas regulators should be purchased for future Thermo-Gravimetric testing that utilizes high-pressure bottled purge gas.
3. The isothermal hold time for the tests in air at 260 and 288 °C should be increased in order to increase the level of confidence that the specimens reached a constant rate of normalized weight loss.
4. A third test in oxygen at 343 °C should be conducted with a larger specimen size in an effort to determine whether a constant rate of weight loss can be reached and to validate or invalidate the hypothesis that the abrupt, high initial weight loss observed was anomalous.

5. The third 343 °C test in oxygen should be used to refine the Time-Temperature Superposition Master curve for oxygen.
6. Future neat resin powder testing should use consistent 110 °C moisture hold times to remove subjectivity from the data.

Appendix A: Unsmoothed Rates of Weight Loss for Air and Argon

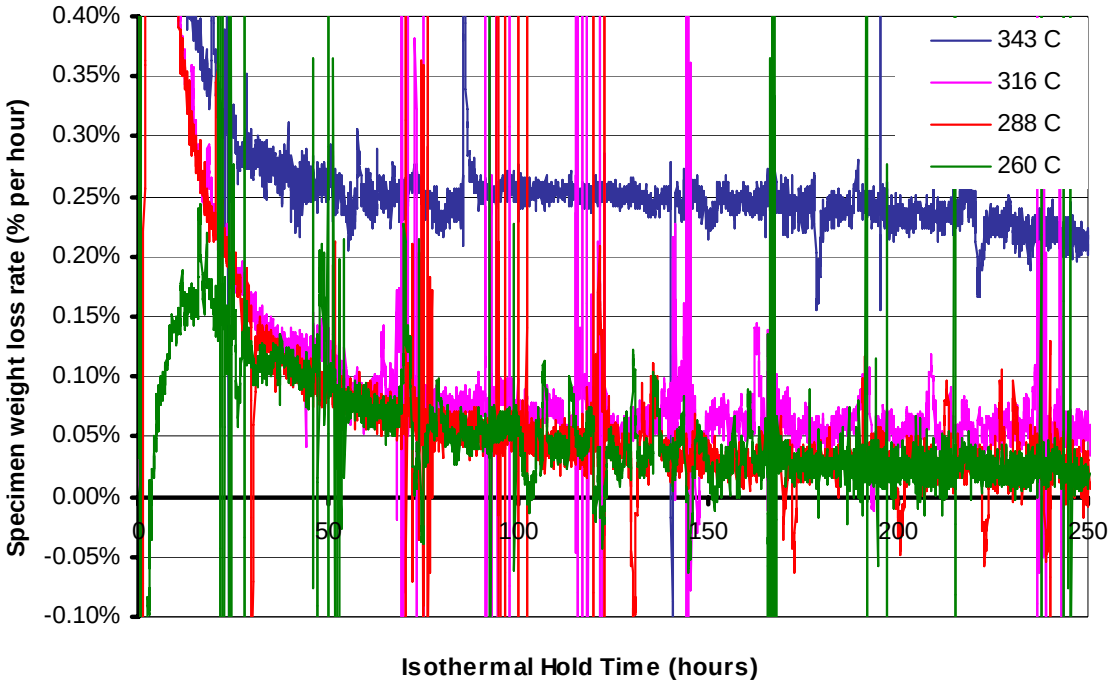

Figure 45: Rate of Normalized Weight Loss in Air (no smoothing)

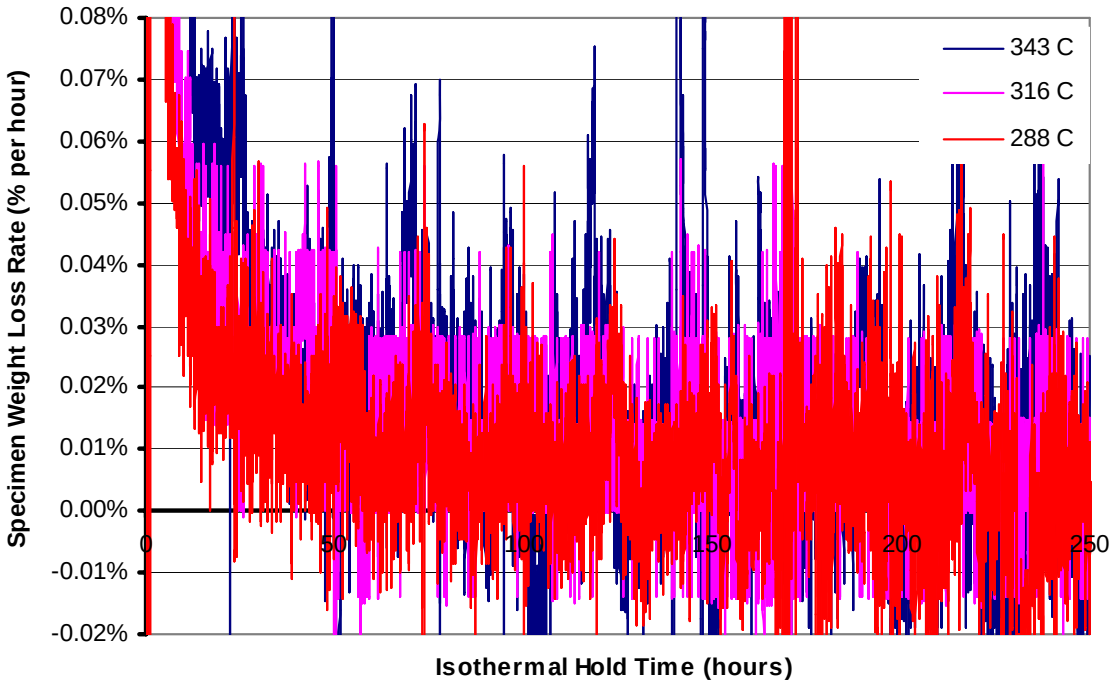

Figure 46: Rate of Normalized Weight Loss in Argon (no smoothing)

Appendix B: Mathcad™ Worksheet Thermo-Oxidative Modeling Effort

MathCad Worksheet for calculation of Modeling parameters used by Pochiraju and Tandon (23)

Calculation of normalizing parameter for the reduction in reaction rate model: Eq. (5)

Weight loss Ratio's: Average value over the linear range as outlined in chapter 3 section 2 part 4

$W_{L\_343} := .549 \qquad W_{L\_316} := .594 \qquad W_{L\_288} := .745$

Oxygen Concentrations for air and pure oxygen

$C_{02} := 3.74 \qquad C_{air} := 0.79$

Solving for the Beta values

$Ratio := W_{L\_343}$ Change the definition to the appropriate temperature and then read off the positive real Beta value from below.

$$Beta(\beta) := \frac{2\cdot\beta\cdot C_{air}}{1+\beta\cdot C_{air}}\cdot\left[1-\frac{\beta\cdot C_{air}}{2\cdot(1+\beta\cdot C_{air})}\right] - Ratio\cdot\frac{2\cdot\beta\cdot C_{02}}{1+\beta\cdot C_{02}}\cdot\left[1-\frac{\beta\cdot C_{02}}{2\cdot(1+\beta\cdot C_{02})}\right]$$

$$Beta(\beta)\ solve,\beta \rightarrow \begin{pmatrix} 0 \\ -3.1408513702172820106 \\ -.41631963305307292618 \\ .49076607536133171873 \end{pmatrix}$$

Determination of the Saturation Reaction Rate

Constants provided by G.P. Tandon, Contractor for AFRL/Materials Directorate

$$R_a := 23379.63\,\frac{J}{mol} \qquad R_{0S} := 536.94\,\frac{mol}{m^3\cdot min} \qquad R := 8.31447\,\frac{J}{mol\cdot K}$$

Temperatures of Interest

$$T := \begin{pmatrix} 288+273 \\ 316+273 \\ 343+273 \end{pmatrix}\cdot K$$

Arrhenius-type Relation for Saturation Reaction Rate

$$R_0 := R_{0S}\cdot e^{\frac{-R_a}{R\cdot T}} \qquad R_0 = \begin{pmatrix} 3.574 \\ 4.535 \\ 5.591 \end{pmatrix}\frac{mol}{m^3 min}$$

Determination of the proportionality constant alpha

Reduction in Reaction Rate Function

$$\beta_0 := \begin{pmatrix} 1.114 \\ 0.594 \\ 0.491 \end{pmatrix} \frac{m^3}{mol} \qquad C_{air} := .79 \frac{mol}{m^3} \qquad \text{Constants from above}$$

$$\frac{2 \cdot \beta_0 \cdot C_{air}}{1 + \beta_0 \cdot C_{air}} \cdot \left[1 - \frac{\beta_0 \cdot C_{air}}{2 \cdot \left(1 + \beta_0 \cdot C_{air} \right)} \right] = 1.735 \qquad f_c := \begin{pmatrix} .717 \\ .537 \\ .481 \end{pmatrix}$$

Weight loss rates: taken from test data

$$dW\_dt_{air\_linear} := \begin{pmatrix} 0.00027 \\ 0.00061 \\ 0.00242 \end{pmatrix} \frac{1}{hr} \qquad dW\_dt_{argon\_linear} := \begin{pmatrix} 0.000019 \\ 0.000069 \\ 0.000099 \end{pmatrix} \cdot \frac{1}{hr}$$

PMR-15 Material Properties: density take from (4)

$$M := 1500 \frac{gm}{mol} \qquad \rho_{un} := 1.3 \frac{gm}{cm^3} \qquad \rho_{ox} := 1.3 \frac{gm}{cm^3}$$

Molar weight is of unoxidized material.
This will be different for the oxidized material.

Long Term steady state proportionality constant

$$\alpha := \frac{\left(dW\_dt_{air\_linear} - dW\_dt_{argon\_linear} \right) \cdot \rho_{un}}{\overrightarrow{\left(R_0 \cdot f_c \right)} \cdot M}$$

$$\alpha = \begin{pmatrix} 1.415 \times 10^{-3} \\ 3.209 \times 10^{-3} \\ 0.012 \end{pmatrix}$$

Bibliography

1. Meador, Michael A. "Recent Advances in the Development of Processable High-Temperature Polymers," *Annual Review of Material Science*, 28: 599-630 (1998).

2. Mendenhall, Susan, P. *Thermo Gravimetric Analysis of PMR-15 Neat Resin*, MS Thesis, AFIT/GAE/ENY/04-J08. School of Engineering and Management, Air Force Institute of Technology, Wright-Patterson AFB OH, June 2004.

3. "DMBZ Polyimides Provide an Alternative to PMR-15 for High-Temperature Applications," NASA Lewis Research Center – http://www.grc.nasa.gov/WWW/RT1995/5000/5150c.htm

4. Marais, C., D. Leveque, A. Schieffer, and X. Colin. "Multidisciplinary Effects of Aging Factors on Damage in Structural Composites," *International Conference on Composite Materials-ICCM 14*, San Diego CA, July 2003.

5. Bowles, K.J., L.S. McCorkle and L.S. Ingraham. "Comparison of Graphite Fabric Reinforced PMR-15 and Avimid N Composites After Long Term Isothermal Aging at Various Temperatures," NASA TM 1998 – 107529, February 1998.

6. Ripberger, E.R., G.P Tandon and G.A. Schoeppner. "Characterizing Oxidative Degradation of PMR-15 Resin," AFRL/Material and Manufacturing Directorate, Wright-Patterson AFB OH.

7. Schoeppner, G.A. and D.B. Curliss. "Model-Based Design for Composite Materials Life Management," AFRL/Materials and Manufacturing Directorate, Wright-Patterson AFB OH.

8. Bowles, K.J., D.S. Papadopoulos, L.L. Inghram, L.S. McCorkle and O.V. Klan. "Longtime Durability of PMR-15 Matrix Polymer at 204, 260, 288, and 316 ˚C," NASA TM 2001 – 210602, July 2001.

9. Bowles, K.J. "Thermal and Mechanical Durability of Graphite-Fiber-Reinforced PMR-15 Composites," NASA TM 1998 – 113116/REV1, July 1998.

10. Bowles, K. J., A. Meyers. "Specimen geometry effects on graphite/PMR-15 composites during oxidative aging," *32nd Int. SAMPLE Symposium and Exhibition*, 1285, 1986.

11. Bowles, K.J., M. Madhukar, D.S. Papadopolous, L.S. Ingram and L.S. McCorkle. "The Effects of Fiber Surface Modification and Thermal Aging on Composite Toughness and Its Measurement," NASA TM 1995 – 106765, May 1995.

12. Chung, K., J.C. Seferis, J.D. Nam. "Investigation of thermal degradation behavior of polymeric composites: prediction of thermal cycling effect from isothermal data," *Composites*: Part A 31, 945-957, (2000).

13. Meador, Mary Ann B., Aryeh A. Frimer. "Approaches to New Endcaps for Improved Oxidation Resistance." *Polymer Preprints*, 41(1), 283, (2000).

14. Xie, Wei, Wei-Ping Pan, Kathy C. Chuang. "Thermal Characterization of PMR polyimides," *Thermochimica Acta*, 143-153, (2001).

15. Patekar, Kaustubh A., *Long Term Degradation of Resin for High Temperature Composites*, MS Thesis, School of Engineering, Massachusetts Institute of Technology, Boston MA, 1998.

16. Tsuji, L.C., H.L McManus and K.J Bowles. "Mechanical Properties of Degraded PMR-15 Resin," NASA TM 1998 – 208487, August 1998.

17. Johnson, Lili L., R.K. Eby, Mary Ann B. Meador. "Investigation of oxidation profile in PMR-15 polyimide using atomic force microscope (AFM)," *Polymer*, 44, 187-197, (2003).

18. Pochiraju, K. V., G. P. Tandon. "Modeling Thermo-Oxidative Layer Growth in High-Temperature Resins," accepted to *Journal of Engineering Materials and Technology*, (April 2005).

19. Abdeljaoued, K. *Thermal Oxidation of PMR-15 Polymer Used as a Matrix in Composite Materials Reinforced with Carbon Fibers*, PhD Dissertation, Ecole Nationale Superieure des Arts et Metiers, Paris France, 1999.

20. Schoeppner, G.A. and G.P Tandon. "Aging and Durability of PMR-15 High Temperature Polyimide," AFRL/Materials and Manufacturing Directorate, Wright-Patterson AFB OH.

21. IPCS INCHEM, "Chemical Safety Information from Intergovernmental Organizations," www.inchem.org/documents/icsc/icsc/eics0024.htm, April 2000.

22. Reeder, James, A. "Prediction of Long-Term Strength of Thermoplastic Composites using Time-Temperature Superposition," NASA/TM-2002-211781, August 2002.

Vita

Ensign Grant W. Robinson graduated from W.T. Woodson High School in Fairfax, VA. After graduation, he began undergraduate studies at Maine Maritime Academy located in Castine, Maine where he graduated with a Bachelor of Science degree in Marine Systems Engineering in May 2003. He was commissioned through the Maine Maritime Academy Naval Reserve Officer Training Corps Program (MMANROTC) located at Maine Maritime Academy.

In June 2004, his first assignment was at Wright-Patterson Air Force Base in Dayton, Ohio where he entered the Graduate School of Engineering and Management, Air Force Institute of Technology. Upon graduation in June 2005, he will be assigned to Naval Air Station Pensacola in Pensacola, Florida where he will be enrolled as a student aviator.

REPORT DOCUMENTATION PAGE

Form Approved
OMB No. 074-0188

1. REPORT DATE *(DD-MM-YYYY)*	**2. REPORT TYPE**	**3. DATES COVERED** *(From – To)*
13-06-2005	**Master's Thesis**	July 04 – Jun 05

4. TITLE AND SUBTITLE

High Temperature Chemical Degradation of PMR-15 Polymer Resins

5a. CONTRACT NUMBER

5b. GRANT NUMBER

5c. PROGRAM ELEMENT NUMBER

6. AUTHOR(S)

Robinson, Grant W., Ensign, USN

5d. PROJECT NUMBER
JON 286

5e. TASK NUMBER

5f. WORK UNIT NUMBER

7. PERFORMING ORGANIZATION NAMES(S) AND ADDRESS(S)
Air Force Institute of Technology
Graduate School of Engineering and Management (AFIT/EN)
2950 Hobson Way
WPAFB OH 45433-7765

8. PERFORMING ORGANIZATION REPORT NUMBER

AFIT/GAE/ENY/05-J09

9. SPONSORING/MONITORING AGENCY NAME(S) AND ADDRESS(ES)
AFRL/Materials and Manufacturing Directorate
Attn: Dr. Greg Schoeppner
2941 Hobson Way
WPAFB OH 45433-7750 DSN: 59072 PHONE: (937) 255-9072

10. SPONSOR/MONITOR'S ACRONYM(S)

11. SPONSOR/MONITOR'S REPORT NUMBER(S)

12. DISTRIBUTION/AVAILABILITY STATEMENT
APPROVED FOR PUBLIC RELEASE; DISTRIBUTION IS UNLIMITED

13. SUPPLEMENTARY NOTES

14. ABSTRACT

PMR-15 is a polymer resin for glass and carbon reinforced composites used for high temperature, civilian and military aerospace applications. The harsh environments of PMR-15 applications lead to long term structural degradation and, in turn, impact the readiness capabilities of the system. This study investigated the thermal and oxidative degradation of PMR-15 neat resin powder through the use of thermal gravimetric analysis (TGA) in oxygen, argon and air at isothermal hold temperatures of 260, 288, 316, and 343 °C for 250 hours. The TGA measured the degradation by recording the change in neat resin powder mass versus time. The qualitative results were similar for all tests. The specimens initially lost weight at a rapid rate followed by a reduction in the weight loss rate to a near constant value that was dependent upon the isothermal temperature and the gaseous environment. The data from these tests will be used by researchers in the Air Force Research Laboratory Materials and Manufacturing Directorate to further efforts made towards developing a constitutive law and the associated models to predict the behavior of polymer matrix reinforced composites.

15. SUBJECT TERMS
Thermogravimetric Analysis, Composite Materials, Thermal Degradation, Matrix Materials, Thermo-Oxidative Aging

16. SECURITY CLASSIFICATION OF:			**17. LIMITATION OF ABSTRACT**	**18. NUMBER OF PAGES**	**19a. NAME OF RESPONSIBLE PERSON**
REPORT	**ABSTRACT**	**c. THIS PAGE**			ANTHONY N PALAZOTTO, ENY
U	**U**	**U**	**UU**	91	**19b. TELEPHONE NUMBER** *(Include area code)* (937) 255-6565, e-mail: ANTHONY.PALAZOTTO@afit.edu

Standard Form 298 (Rev: 8-98)
Prescribed by ANSI Std. Z39-18